U.PORTO

FACULDADE DE CIÊNCIAS
UNIVERSIDADE DO PORTO

Identification of novel non-muscle myosin IIA (NMIIA) interacting partners

Marina Patrícia Fonseca Santos
Faculdade de Ciências da Universidade do Porto
Mestrado em Biologia Celular e Molecular
2013

U.PORTO

FACULDADE DE CIÊNCIAS
UNIVERSIDADE DO PORTO

Identification of novel non-muscle myosin IIA (NMIIA) interacting partners

Marina Patrícia Fonseca Santos

Porto
2013

Identification of novel non-muscle myosin IIA (NMIIA) interacting partners

Marina Patrícia Fonseca Santos
Mestrado em Biologia Celular e Molecular
Departamento de Biologia
2013

Orientadora
Sandra Sousa, PhD, Instituto de Biologia Molecular e Celular da Universidade do Porto
Co-Orientador
Francisco Mesquita, PhD, Instituto de Biologia Molecular e Celular da Universidade do Porto

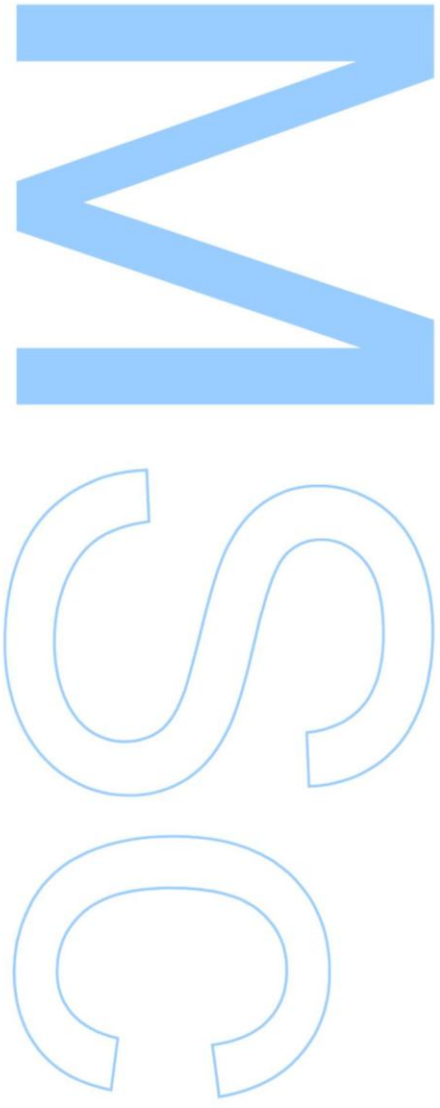

U.PORTO

FACULDADE DE CIÊNCIAS
UNIVERSIDADE DO PORTO

Todas as correções determinadas pelo júri, e só essas, foram efetuadas.

O Presidente do Júri,

Porto, _____/_____/_____

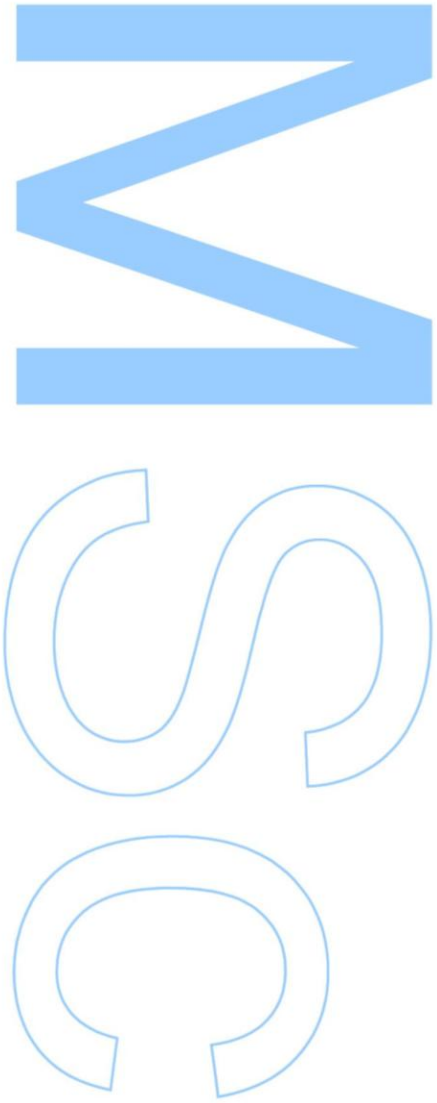

Dissertação de candidatura ao grau de Mestre em Biologia Celular e Molecular submetida à Faculdade de Ciências da Universidade do Porto.

O presente trabalho foi desenvolvido sob a orientação científica da Doutora Sandra Sousa, no Instituto de Biologia Molecular e Celular da Universidade do Porto.

Dissertation for applying to a Master's Degree in Cell and Molecular Biology, submitted to the Faculty of Sciences of the University of Porto.

The present work was developed under the scientific supervision of Doctor Sandra Sousa and was done at the Institute for Molecular and Cell Biology.

Acknowledgments

A most sincere thank you to Doctor Didier Cabanes, who afforded me the opportunity to do my master's project in his laboratory. This past year has allowed me to grow both as a person and as a researcher.

My next thank you is addressed to Doctor Sandra Sousa, for having me as a part of her sub-group inside the group of 'Molecular Microbiology' for this past year and for always making me feel welcome. For always being available to listen and offer suggestions about work and advice about how to improve myself as a researcher and as a part of a research group. I will take the advice to heart.

I would also like to thank Doctor Francisco Mesquita for all the time he spent working and developing this project with me, for all the support he gave me, for always being ready to listen to me (even though I don't speak so much) and explain anything and everything I had doubts about. For his guidance and advice, for always trying to point me in the right direction and for acting not only as my supervisor but as my friend.
I will take with me for the rest of my life and career your work ethic, your dedication and perseverance and your enthusiasm for making science. So I think the only thing left to say is: Thank you so very much Francisco (I really do mean it).

To all my colleagues in the group of 'Molecular Microbiology': Rui Cruz, Rita Pombinho, Jorge Pinheiro, Claúdia Brito, Ana Vieira, Ana Costa, Filipe Carvalho, Paulo Cunha, Teresa Almeida, Sandra Reis, Zóe Virion and Elsa Leitão. Thank you for your kindness, for all the good moments, for all the help and advice that you gave me that were invaluable during the realization of this project and that I am sure will help me for the rest of my career, wherever it will take me.

I would also like to thank Professor José Pissarra for his mentoring, kindness and availability whenever his help was requested.

To my all my closest friends my most sincere thank you.

Mariana, I’m really sorry for all the times you had to listen to me talk about myosin, proteins, IPs and whatever else was on my mind. Thank you for always being there for me. I’m extremely grateful for having you as my friend.

Sofia, I can’t thank you enough for everything. For always being there, for the talks and laughs over coffee and lunch, for the sage advice, for the musical suggestions and simply for being my friend.

I want to give a very special thank you to all my family for their words of incentive and strength and for always believing in me. To my cousin Bruna: thank you for being you, for caring so much and for all the motivation you give me.

And last but definitely not least I want to give a most heartfelt and gigantic thanks to my mom and dad. The two of you taught me to never give up. Without you I would have never been where I am today. Thank you for giving me the opportunity to be doing what I’m doing. Thank you for letting me rant about work and for actually listening to me. Thank you for loving me unconditionally, for believing in me so much and for always giving me so much strength. Thank you for everything. I love you.

Resumo

A miosina-IIA (NMIIA) pertence a uma família de proteínas-motoras que estão associadas a processos que requerem força e motilidade. Esta proteína é capaz de se ligar à actina. Por intermédio desta interação a NMIIA media o movimento dependente da actina e intervém em vários processos celulares como a divisão, migração, polaridade e a estabilidade do citoesqueleto.
A NMIIA também está envolvida em transporte de vesiculas no interior da célula, nomeadamente no transporte retrógrado de proteínas do Golgi para o Retículo Endoplasmático para sofrerem degradação pelo proteosoma.

No nosso laboratório a miosina é estudada num contexto de infeção bacteriana e em condições fisiológicas normais. Resultados obtidos anteriormente pelo nosso laboratório demonstram que a depleção da NMIIA, usando *small interference* RNA (siRNA), favorece a invasão das células hospedeiras por *Listeria monocytogenes*.

Um *yeast two-hybrid* foi realizado como ponto de partida para aprofundar o nosso conhecimento acerca desta proteína, começando pela análise dos seus possíveis parceiros de interação. Dos 97 resultados obtidos no *yeast two-hybrid* selecionamos 5 para testar a sua interação com a NMIIA por métodos bioquímicos. Dos 5, 2 distinguiram-se, tornando-se relevantes para o projeto em realização. Foram a beta-adaptina e *heat shock protein 56.*

Uma possível associação entre a NMIIA e a beta-adaptina e a NMIIA e *heat shock protein 56* foi observada durante a realização do projeto. Esta possível associação foi identificada por imunoprecipitação. A identificação de um mecanismo fisiológico e funcional dependente desta interação em condições fisiológicas normais e num contexto de infeção bacteriana é o passo seguinte deste projeto.

Com este projeto esperamos aumentar o nosso conhecimento acerca da NMIIA e da sua influência na regulação do citoesqueleto, no transporte de vesículas no interior da célula e acerca do seu papel em infeções bacterianas.

Palavras-chave: miosina IIA, *yeast two-hybrid*, parceiros de interação, beta-adaptina e *heat shock protein 56*

Abstract

Non-muscle myosin-IIA (NMIIA) belongs to an ATP-dependent family of motor-proteins mainly involved in processes that require force and motility. This molecule is capable of binding to actin. Via this interaction NMIIA mediates contractility and actin-based motility. Thus NMIIA is capable of mediating several key cellular functions such as: division, migration, polarity and cytoskeletal stability.
NMIIA is also involved in intracellular vesicular transport, including retrograde transport of cargo from the Trans-Golgi Network (TGN) back to the Endoplasmic Reticulum (ER) to undergo proteosomal degradation.
In our laboratory we study NMIIA functions both in infection and regular physiological conditions. Previous work from our laboratory demonstrated that depletion of NMIIA by siRNA favoured the invasion of host cells by *Listeria monocytogenes*.

Given the involvement of this protein in cytoskeleton regulation and infection it is in our interest to increase our knowledge about it. A yeast two-hybrid (Y2H) screen was performed as a starting point to study NMIIA and its interacting partners.
Out of 97 positive interactions we selected 5 putative interactive partners and used biochemical techniques to confirm their association with NMIIA. From the five a total of two became increasingly relevant through the realization of this project: beta-adaptin and heat-shock protein 56 (Hsp56).

Throughout the work performed in the framework of this project we observed a possible association between NMIIA and Hsp56 and also between NMIIA and beta-adaptin. This possible association was suggested by the results obtained using immunoprecipitation (IP). Discovery of a functional and physiological role for these possible NMIIA interacting partners, in a regular physiological context and in an infection context, is the next step in this project.

We expect our work will allow a better understanding of NMIIA and therefore increase our knowledge about the influence of this protein on cytoskeleton regulation, intracellular vesicular transport and ultimately bacterial infection.

Key words: non-muscle myosin IIA, yeast-two hybrid, interacting partners, beta-adaptin and heat-shock protein 56

Table of Contents

List of Figures

List of Tables

Abbreviations

ADP	Adenosine Diphosphate
AFF1	AF4/FMR2 family member 1
AP1 to AP4	Adaptor protein complexes 1 to 4
ALF	AF4/LAF4/FMR2
aPKC	Apical Protein Kinase C
ATP	Adenosine Triphosphate
BSA	Bovine Serum Albumine
C2GnT-M	Core 2 N-acetylglucosaminyltransferase-M
CAR	Coxsackie Adenovirus Receptor
CCV	Clathrin-coated vesicle
CDC	Center for Disease Control and Prevention
CK2	Casein Kinase 2
co-IP	co-Immunoprecipitation
CTLA-4	Cytotoxic T-Lymphocyte Antigen 4
DMSO	Dimethyl sulfoxide
DMEM	Dulbecco's Modified Eagle Medium
EDTA	Ethylenediamine tetraacetic acid
ELC	Essential Light Chain
EMEM	Eagle’s Minimum Essential Medium
ER	Endoplasmic Reticulum
FCS	Fetal Calf Serum
FKBP	FK506-binding proteins
FS	Forwad scatter
gB and gD	Glicoproteins B and D
Hsp56	Heat-shock protein 56
Hsp70	Heat-shock protein 70
Hsp90	Heat-shock protein 90
HSV-1	Herpes simplex virus 1
kDa	kilo-Dalton
KRAB	Krüppel associated box
KSHV	Kaposi’s Sarcoma-Associated Herpersvirus
LB	Luria Broth
LLO	Listeriolysin O

MDCK	Madin-Darby Canine Kidney
MPR	Mannose Phosphate Receptor
MTOC	Microtubule Organizing Center
NCBI	National Center for Biotechnology Information
NEAA	non-essential amino-acids
NMHCII	Non-muscle myosin II heavy chains
NMII	Non-muscle myosin II
NR1	N-Methyl-D-aspartate (NMDA) receptor subunit 1
PBS®	Predicted Biological Score
PFA	paraformaldehyde
RLC	Regulatory Light Chain
ROS	Reactive Oxygen Species
SDS	Sodium dodecyl sulfate
SMPD4	sphingomyelin phosphodiesterase 4
SOD	Superoxide dismutase
TAD	transactivation domain
TGN	Trans-Golgi Network
VSVG	Vesicular stomatitis virus G protein
Y2H	Yeast two-hybrid
ZNF12	Zing-finger protein 12

1. Introduction

1.1 Cell cytoskeleton

To maintain its shape and structure each cell has an organized filament network designated cytoskeleton. Three cytoskeletal filament classes can be distinguished: microtubules, intermediate filaments and actin filaments.

Microtubules are tubular polymers formed by dimers of alpha and beta tubulin that can reach 25 nm in length. Microtubules are organized in microtubule organizing centers (MTOC) and occupy the length of the cell providing mechanical support. Microtubules are anchored to the MTOC by their minus end while their plus end continues to grow at the cell periphery. These filaments have a hollowed structure and can form tightly aligned bundles that act as tracks for the transport of intracellular vesicles. To move cargo along microtubules is necessary the binding of motor proteins. Kynesin is the most common motor binding microtubules and promotes movement of cargo towards the plus end of the filament. Dynein also binds microtubules to move cargo towards their minus end. In cell division they are responsible for the formation of the mitotic spindle (Alberts et al., *Molecular Biology of the Cell*, 2008).

Intermediate filaments are dynamic filaments with an average diameter of 10 nm and are organized in a diffuse mesh throughout the whole cytoplasm allowing maintenance of cell shape and providing mechanical strength. They are composed of a variety of proteins that are organized in 5 groups: types I and II correspond to keratins; type III include vimentin and desmin; type IV correspond to three neurofilament proteins and type V are components of the nuclear envelope, designated lamins. In epithelia these cytoskeletal filaments can interact with proteins at cell-cell junctions promoting adhesion and creating a cohesive cell layer (Alberts et al., *Molecular Biology of the Cell*, 2008; Cooper, *The Cell: a molecular approach*, 2000).

Actin filaments, also named microfilaments, are the smaller cytoskeletal filaments with an average 7 nm diameter. Actin can be present as a monomer designated G-actin or as part of a microfilament called F-actin. It is involved in various cellular processes: motility, vesicle movement, cell signaling, cell division, cytokenesis and muscle contraction. These filaments are flexible structures disperse throughout the cell cortex with a higher concentration just beneath the plasma membrane providing strength and shape to the lipid bilayer. Actin can produce movement by itself or through association with motor protein myosin. Actin is capable of forming dynamic cellular projections, like

the lamellipodia, essential to cell motility. These projections occur at the leading edge of migrating cells and are comprised of dense actin filaments and accessory proteins that undergo cycles of remodeling in order to rapidly respond to outside stimuli and surface receptors (Grantham et al., 2012; Alberts et al., *Molecular Biology of the Cell*, 2008).

Actin filaments, microtubules and intermediate filaments are capable of interacting with molecular motors: kynesin, dynein and myosin (Alberts et al., *Molecular Biology of the Cell*, 2008; Helfand et al., 2003). Molecular motors can be defined as molecules responsible for force transduction, meaning the conversion of chemical energy into mechanical energy.

1.2 Myosins

Myosins are a large superfamily of molecular motors present in all eukaryotic cells and capable of associating with actin. They are ATP-dependent motor proteins that are involved in various cellular processes that require force and motility (Vicente-Manzanares et al., 2009).

Myosins are typically constituted by three subdomains: the N-terminal well-conserved motor or head domain, the neck domain and the C-terminal class-specific tail domain. The tail domain presents the biggest variations between myosin classes, varying in length and amino acid composition and is thought to play distinguishable roles in class-specific functions (Sellers, 2000; Landsverk and Epstein, 2005).

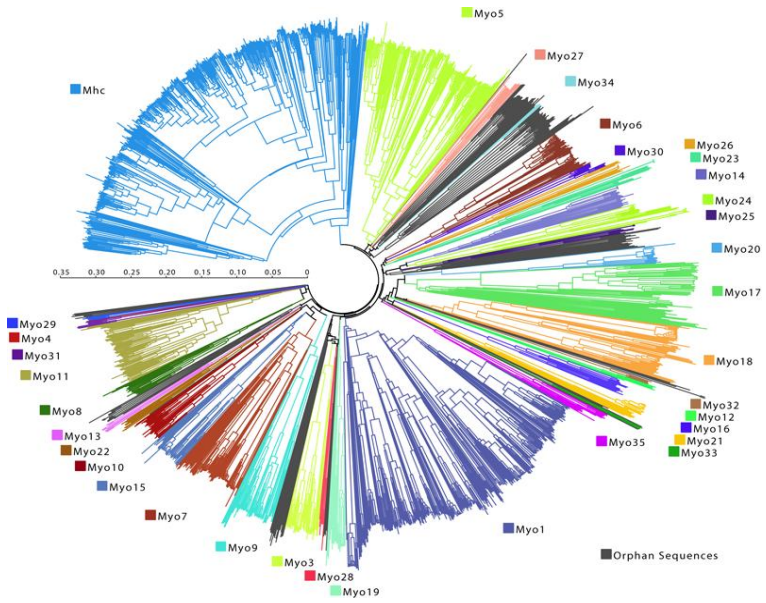

Figure 1 Phylogenetic tree constructed from analysis of the motor domains of 1984 myosins. Based on this phylogenetic analysis 35 myosin classes have been identified. Branches colored in black correspond to unclassified myosins. Adapted from Motorprotein.de 2007

The variable tail domain is thought to determine cellular localization, filament assembly and differential cargo binding. There are at least 35 different classes in the myosin superfamily determined by analysis of their motor domain (Figure 1). Myosins are encoded by 25 genes and distinct

isoforms can occur due to alternative splicing of mRNA (Sellers, 2000; Conti and Adelstein, 2008).

1.3 Myosin II

The myosin II subfamily is also designated as conventional myosins. Members of the class II are constituted by 6 polypeptides: two heavy chains (NMHCII) of 230 kDa that form the head and tail domains. Tail domain possesses coiled-coil regions that support dimerization of the molecule creating two globular heads. The intermediate region between myosin's head and tail is denominated neck and binds two regulatory light chains (RLC) of 20 kDa and two essential light chains (ELC) of 17 kDa (Figure 2). The RLC allow myosin regulation through phosphorylation and the ELC stabilize the structure of the protein (Sellers, 2000; Landsverk and Epstein, 2005). This subfamily is the largest and encompasses skeletal, cardiac and smooth muscle myosins as well as the non-muscle myosin II (NMII). There is one main difference between the members of the myosin II class. While skeletal and cardiac muscle myosin II is regulated by troponin and tropomyosin (actin-associated proteins), the regulation of non-muscle and smooth muscle myosin is achieved primarily through phosphorylation of the RLC (Conti and Adelstein, 2008).

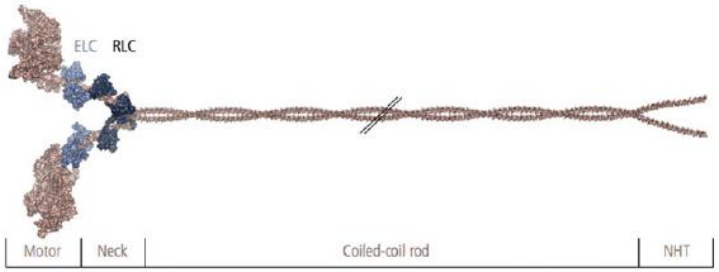

Figure 2 Representation of the myosin II class molecule. Depicted are the three main domains (motor, neck and tail comprising the coiled-coil rod and the non-helical tail) and the three pairs of chains that constitute the hexamer (heavy chains, ELC and RLC). Adapted from Heissler and Manstein, 2013.

The actin-binding and subsequent ATP hydrolysis in the myosin II head domain generates energy that will allow myosin to propel itself towards the plus end of an actin filament and generate movement. In skeletal muscle the myosin-dependent ATP-induced sliding of actin filaments results in the generation of contraction (Alberts et al., *Molecular Biology of the Cell*, 2008).

1.4 Non-muscle myosin II (NMII)

Non-muscle myosins are the most abundant group of molecular motors in eukaryotic cells and are present in both muscle and non-muscle cells. NMII are essential for cell

migration, adhesion, shape changes, cytokinesis, endocytosis and exocytosis. This subfamily acts as a regulator of the actin cytoskeleton constituting a network designated as actomyosin. This network is capable of responding to extra and intracellular stimuli and generates movement according to the demands of the cell. Three distinct NMII isorforms were identified on mammalians termed NMIIA, NMIIB and NMIIC, encoded by *Myh9*, *Myh10* and *Myh14* genes, respectively. Although these three isoforms share 60 to 80 % of their amino acid composition they have isoform-specific functions (Bresnick, 1999; Conti and Adelstein, 2008; Vicente-Manzanares et al., 2009; Betapudi, 2010; Wang et al., 2011; Heissler and Mainstein, 2013). The rate of ATP hydrolysis and the amount of time the myosin-actin interaction occurs during the contractile cycle (duty ratio) are very different between isoforms (Wang et al., 2011; Vicente-Manzanares et al., 2009). NMIIB has a higher duty ratio and high affinity to ADP when compared to NMIIA. This isoform is capable of exerting tension for longer periods of time spending less energy than NMIIA (Vicente-Manzanares et al., 2009). The formation of bipolar filaments by the tail domain is a mechanism used to maintain tension on actin filaments for prolonged time periods. The maintenance of tension on actin filaments by the bipolar filaments is a mechanical and structural function that is mainly separate from the enzymatic activity of the motor domain and can be performed by the three different NMII isoforms (Figure 3) (Conti and Adelstein, 2008; Wang et al., 2011).

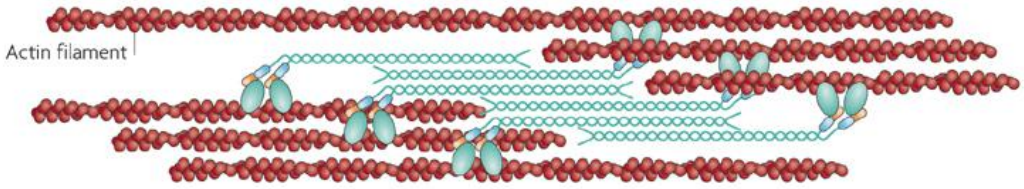

Figure 3 Formation of bipolar filaments by NMII. By interactions of the rod domain NMII molecules assemble into bipolar filaments that are capable of exerting tension on actin filaments for prolonged time periods. Adapted from Vicente-Manzanares et al., 2009.

Furthermore opposite roles for NMIIA and NMIIB in lamellipodia extension during cell spreading have been described. Depletion by siRNA of NMIIB reduced the rate of lamellipodia extension while NMIIA depletion increased this rate, suggesting that each molecule generates tension in opposite directions (Betapudi, 2010). The role of the NMIIC isoform in lamellipodia extension or retraction is not yet defined (Heissler and Manstein, 2013).

1.5 NMIIA

NMIIA acts as an integrator of cellular processes such as cell migration, polarity, division, adhesion, tissue architecture and cytoskeletal coherence (Cai et al., 2009), through its binding with cytoskeletal actin. Out of the three isoforms of NMII, NMIIA has the highest rate of ATP hydrolysis and propels actin faster than NMIIB and NMIIC (Vicente-Manzanares et al., 2009). Regulation of NMIIA activity is done by phosphorylation of serine 19 and threonine 18 in the RLC. RLC phosphorylation regulates assembly of NMIIA by preventing intramolecular interactions (head-head and head-tail), which would lead to a closed conformation, and allows the maintenance of the elongated myosin filament (Conti and Adelstein, 2008; Vicente-Manzanares et al., 2009). Various phosphorylation sites are present in the NMIIA heavy chains C-terminal non-helical tail but their relevance is still unknown (Bresnick, 1999; Vicente-Manzanares et al., 2009).

Depletion of NMIIA from cells using siRNA impaired migration but increased lamellar protrusions (Betapudi et al., 2006). NMIIA is also important for apical-basal and front-to-back polarity. Tight junctions are the barrier between the apical and basal compartments in a cell. NMIIA is responsible for the assembly of the tight junction components. In a cell depleted of NMIIA the tight junction is not correctly formed and therefore the cell does not polarize (Conti and Adelstein, 2008). Front-to-back polarity is defined by the start of an actin-dependent protrusion at the front of the cell and a NMIIA-dependent detachment mechanism in the cell rear. If NMIIA is inhibited cells elongate because they are not capable of retracting their rear (Conti and Adelstein, 2008; Vicente-Manzanares et al., 2009). Maintenance of cell-cell adhesions is also impaired by the absence of NMIIA which is responsible for controlling the localization of the components of the tight and adherens junctions (Conti and Adelstein, 2008; Vicente-Manzanares et al., 2009). Genetic ablation of NMIIA in embryonic stem cells and mouse embryos leads to loss of cell-cell adhesion due to the absence of the proteins responsible for constructing the junction from the junction site (Conti et al., 2004).

Besides its well-described role in processes that require force and movement NMII is also involved in other intracellular processes. NMII is required to the assembly of basolateral transport vesicles carrying vesicular stomatitis virus G protein (VSVG) (Musch et al., 1997). It has also been described as intervening in intracellular sorting pathways, including retrograde transport of NR1 and C2GnT-M proteins from the Trans-Golgi Network back to the Endoplasmic Reticulum (ER) to undergo proteosomal

degradation (Vazhappilly et al., 2010; Petrosyan et al., 2012). NMIIA has also been implicated in the secretory pathway. In this pathway NMIIA is involved in approach and fusion. It regulates the actin cytoskeleton to allow vesicle recruitment and movement at the plasma membrane. Once the vesicle reaches the plasma membrane NMIIA is involved in fusion of the vesicular carrier with the plasma membrane (Loubéry and Coudrier, 2008; Bond et al., 2011).

Among other myosin related pathologies, one of the most common conditions is a dysfunction of the blood platelets resulting in a pathology designated macrothrombocytopenia. This pathology is characterized by a reduction on the number of platelets present in the blood, by uncharacteristically large platelets which will lead to an increase of the bleeding time before clotting (Canobbio et al., 2005; Zhang et al., 2011).

1.6 NMIIA and infection

Our group studies the food-borne pathogen *Listeria monocytogenes.* This bacterium is considered an opportunistic pathogen, producing disease mainly in immunocompromised individuals, elders and pregnant women. After ingestion of contaminated food bacteria are able to overcome the intestinal barrier reaching the liver and spleen through the bloodstream. Bacteria are also capable of crossing the blood/brain barrier and in pregnant women the placental barrier (Figure 4A). Bacteria adhere to the surface of the host cell and are internalized reaching the cytoplasm inside a vacuole. Through production of a toxin they are capable of escaping the vacuole and subvert the host cytoskeleton in order to promote intracellular motility and cell to cell spread (Figure 4B) (Cossart and Toledo-Arana, 2008; Cossart, 2011; Camejo et al., 2011).

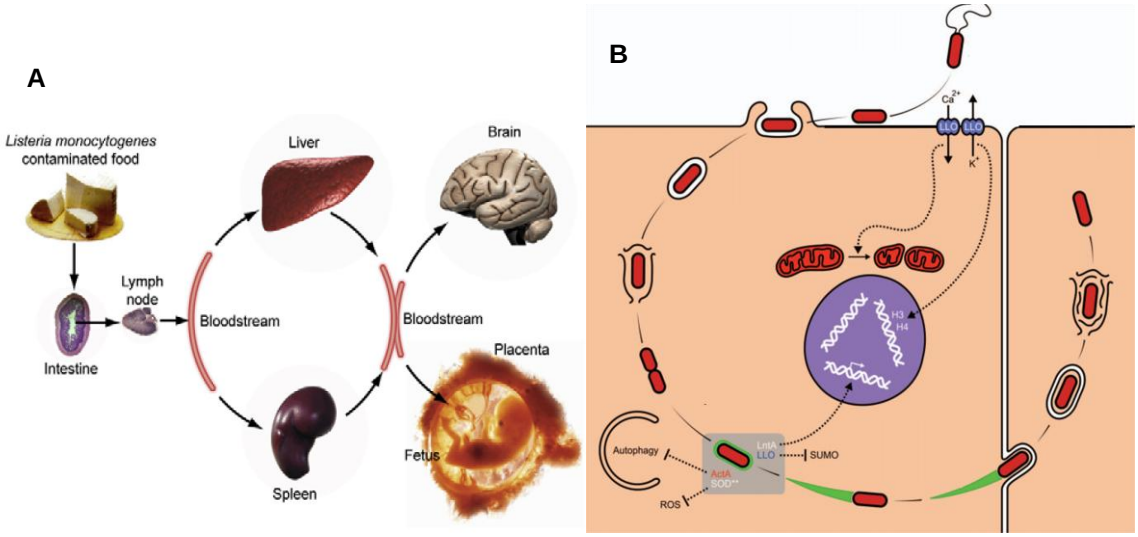

Figure 4 *Listeria monocytogenes* infection cycle *in vivo* and *in vitro* in cultured epithelial cell lines. **(A)** *Listeria monocytogenes* disease dissemination. **(B)** Schematic representation of bacterial intracellular infectious cycle. ROS, reactive oxygen species; SOD, superoxide dismutases; ActA and Listeriolysin O, major *L. monocytogenes* virulence factors; Histone H3 and Histone H4 (A) Adapted from Cossart and Toledo-Arana, 2008 and (B) Adapted from Camejo et al., 2011

Work performed in our laboratory suggested a restrictive role for NMIIA upon *L. monocytogenes* infection. Depletion of NMIIA from host cells led to an increase of *L. monocytogenes* entry levels.

Our group uncovered a new NMIIA post-translational modification, a phosphorylation of the tyrosine residue at position 158 in response to *L. monocytogenes* infection. A NMIIA mutant, where tyrosine residue 158 was replaced by a phenylalanine and therefore incapable of undergoing phosphorylation, was constructed. In host cells expressing the mutant NMIIA isoform *L. monocytogenes* entry was facilitated. This result suggested that tyrosine-phosphorylation of NMIIA acts as a defense mechanism in response to *L. monocytogenes* infection (Almeida et al., submitted).

NMIIA contributes to the invasion of nonphagocytic cells by *Salmonella*. The bacterial protein SopB is capable of activating an invasion mechanism that requires NMIIA to generate membrane ruffling thereby favoring internalization of *Salmonella* (Hänisch et al., 2011).

In addition, NMIIA is involved in viral entry into host cells. Entry of Kaposi's Sarcoma-Associated Herpersvirus (KSHV) is impaired in cells treated with increasing concentrations of blebbistatin (a small-molecule inhibitor with high myosin II affinity that blocks myosin's ATPase activity). Suggesting a NMIIA-dependent entry pathway for KSHV (Veettil et al., 2010).

Herpes simplex virus-1 (HSV-1) entry into host cells requires receptors for glicoproteins B and D (gB and gD). In 2010, NMIIA was characterized as an entry receptor for HSV-1 by interacting with gB. Over-expression of NMIIA increased infection levels by HSV-1

while the use of a specific antibody against NMIIA impaired entry of the virus into host cells (Arii et al., 2010).

Given the relevant role of NMIIA in *L. monocytogenes* infection it was in the interest of our lab to increase our knowledge about this motor protein by uncovering new NMIIA binding partners. The selected methodology was a yeast two-hybrid assay (Y2H).

2. Aims

This project aims to confirm and validate the putative interacting partners of NMIIA revealed by a yeast two-hybrid (Y2H) assay. In addition, we will try to investigate the physiological relevance of the validated interactions in the context of canonical functions of NMIIA. We expect our research to improve our understanding of NMIIA functions and increase our knowledge of eukaryotic cytoskeleton regulation and intracellular vesicular traffic.

We specifically aim to:

- Optimize a protocol for immunoprecipitation (IP) of endogenous NMIIA in HeLa and Jeg-3 cell lines.
- Optimize a protocol for immunoprecipiatation of ectopically expressed NMIIA in HEK 293 cells.
- Evaluate the interactions between NMIIA and the putative interacting partners identified during the Y2H assay by IP.
- Optimize a protocol for immunoprecipitation of the possible interacting partners suggested by the IP-NMIIA in HeLa cells.

3. Material and methods

3.1 Yeast Two-Hybrid Technique (Y2H)

As bait for the Y2H we selected the C-terminal (Leu837 to Glu1960) domain of NMHCII (Figure 5). The tail fragment used as bait was selected for four reasons: the head/motor domain's function and interacting partners, such as actin, are well-described; the motor domain shares the most homology between myosin isoforms, increasing the possibility of sharing binding partners; the tail fragment is the region that presents the most diversity between all myosins and lastly the tail domain possesses different domains that interact with different cytoplasmic proteins e.g. tail domain of myosin VII interacts with vezatin (Karcher et al., 2002). This NMIIA tail fragment was tested against a human placental library. Placentas are developing organs with high expression levels and a high diversity of proteins and are relevant for *L. monocytogenes* pathology.

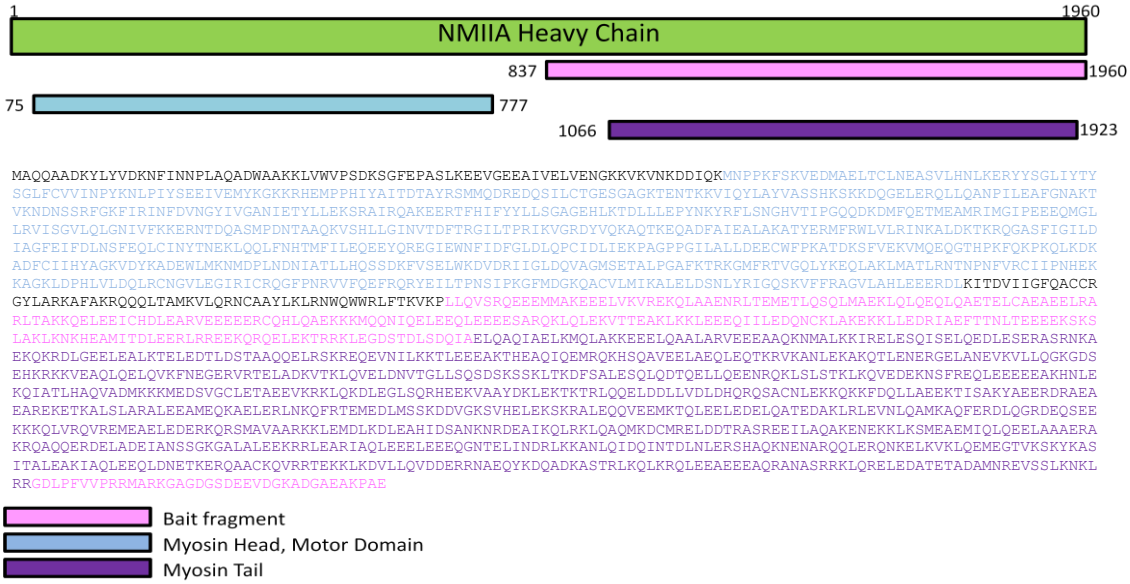

Figure 5 Schematic representation and sequence of the heavy chain of NMIIA. Fragment used as bait for the Y2H is depicted in pink, from leucine 837 to acid glutamic 1960. Motor domain of NMIIA is represented in blue and tail is represented in purple.

The Y2H technique functions as a simple complementation assay. It is based on the premise that in eukaryotic systems activation of transcription depends upon the direct interaction between a binding and activating domains (Dwane and Kiely, 2011).
Therefore in regular physiological conditions the transcription mechanism requires both the DNA-binding and activation domains of a transcription activator (Figure 6A). On the

Y2H system the two domains (DNA-binding and activation domains) are fused to two proteins, a bait protein (in our case the C-terminal domain of NMIIA) and a prey protein (in our case all proteins expressed in placenta). If the two proteins (bait and prey) interact, the DNA-binding and activation domains will bind, form a functional transcription activator and initiate transcription of the reporter gene (Figure 6B). Positive clones are distinguished because they acquire a different color or produce an amino acid that allows their survival in a selective media (Figure 6C) (Dwane and Kiely, 2011).

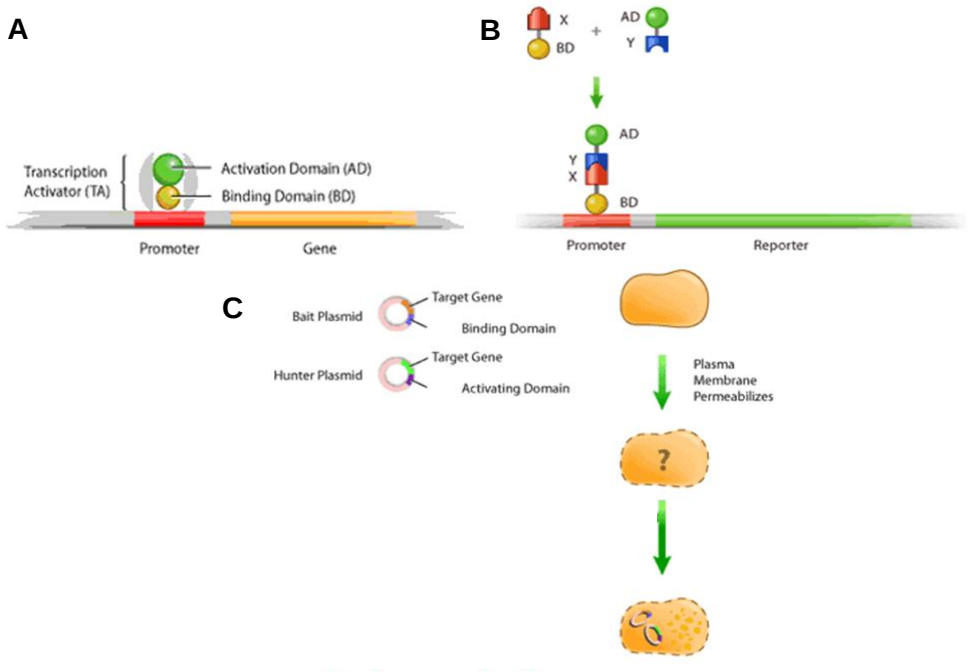

Figure 6 Schematic representation of the Y2H assay. **(A)** Transcription mechanism in regular physiological conditions. **(B)** Y2H system. If binding and activating domains interact transcription is activated. **(C)** Bait and Prey plasmids are transfected into a yeast cell, if interaction occurs colony grows. Adapted from Giorgini and Muchowski, 2005.

The Y2H was performed against a randomly primed cDNA library from human placenta. Positive clones were obtained using a selective media. Identification of the prey fragments of positive clones was done by PCR followed by sequencing. Fragments were analyzed on agarose gel and sequenced at their 5' and 3' sites to ascertain the size and exact positions where the prey fragment interacts with our bait fragment. The obtained sequences were used to identify the corresponding gene, using BLASTN (NCBI), in the GenBank database (NCBI) (Rain et al., 2001; Formstecher et al., 2004).

3.2 Antibodies and plasmids

All antibodies and stains used are described in Table 1. Primary and secondary antibodies as well as molecular probes optimized dilutions for each application are indicated in detail in Table 1. All plasmids used during this study are listed in Table 2.

Table 1 List of antibodies used in this work. Name of the primary and secondary antibodies as well as molecular probes used is listed in the first column. Optimized dilutions for Western Blot (WB), Immunoprecipitation (IP) and Immunofluorescence (IF) are listed for each antibody. Reference and source of each antibody is also described in the table.

Name	*Species*	*Applications*	*Reference*	*Source*
Myosin IIA	Rabbit	WB (1:5000) IP (1:100)	M8064	Sigma-Aldrich
Myosin IIA	Mouse	IF (1:400)	ab55456	Abcam
Myosin IIB	Rabbit	WB (1:1000)	M7939	Sigma-Aldrich
Actin	Mouse	WB (1:5000)	AC-15, A5441	Sigma-Aldrich
GFP	Mouse	WB (1:1000)	B-2, sc9996	Santa Cruz Biotechnology
GFP (Agarose-conjugated)	Mouse	IP (1:100)	B-2, sc-9996 AC	Santa Cruz Biotechnology
β-adaptin	Rabbit	IP (1:100) WB (1:1000) IF (1:50)	H-300, sc-10762	Santa Cruz Biotechnology
SMPD4	Rabbit	WB (1:500)	PA5-25797	Thermo Scientific
Hsp56	Mouse	IP (1:100) WB (1:1000) IF (1:100)	ADI-SRA-1400-D	Enzo Life Sciences
ZNF12	Rabbit	WB (1:1000)	AV35912-100UG	Sigma-Aldrich
AFF1	Rabbit	WB (1:500)	SAB2106246-50UG	Sigma-Aldrich
aPKC-ζ	Rabbit	IF (1:500)	C-20, sc-216	Santa Cruz Biotechnology
Anti-rabbit or anti-mouse HRP	Goat	WB (1:5000)	BI2413C BI2407	PARIS
Anti-mouse Alexa Fluor 488	Goat	IF (1:500)	A11001	Invitrogen
Alexa Fluor 647-conjugated-phalloidin	-	IF (1:50)	A22287	Invitrogen
DAPI	-	IF (1:100)	-	-
Anti-rabbit Cy3	Goat	IF (1:500)	111-165-144	Jackson ImmunoResearch

Table 2 List of plasmids used in this work.

Plasmid Name	Description	Source
GFP-MIIA-WT	pEGFP-C3:CMV-GFP-NMHC IIA	Addgene
GFP-MIIA-Y158F	pEGFP-C3:CMV-GFP-NMHC IIA (Y158F)	Almeida, T. et al, 2013
GFP (C3)	pEGFP-C3	ClonTech Laboratories
GFP-MIIB-WT	pEGFP-C3:CMV-GFP-NMHC IIB	Addgene

3.3 Bacterial strains, cell lines and growth conditions

Escherichia coli (*E. coli*) DH5α and TOP 10 strains were grown aerobically in Luria Bertani (LB) medium (1 % tryptone, 0.5 % yeast extract and 1 % NaCl) (Difco) at 37 ºC with aeration. When necessary ampicilin (100 µg/ml) was added to the culture media.
Human cervical cancer cell line HeLa (ATCC CCL-2), Human embryonic kidney cells (HEK 293) (ATCC CRL-1573) and monkey kidney tissue cells Cos-7 (ATCC CRL-1651) were grown in Dulbecco's Modified Eagle Medium (DMEM) supplemented with 10 % fetal calf serum (FCS). Human placental choriocarcinoma cell line JEG-3 was grown in Eagle's Minimum Essential Medium (EMEM) supplemented with 10 % FCS, 1 % non-essential amino-acids (NEAA) and 1 % sodium pyruvate (NaPyR). Human colorectal adenocarcinoma cell line Caco-2 (ATCC HTB-37) was cultured in EMEM supplemented with 20 % FCS, 1 % NEAA and 1 % NaPyR. Cells were maintained at a confluence of 70 to 80 % at 37 ºC in a 5 % carbon dioxide (CO_2) humidified atmosphere. Cell culture media (DMEM and EMEM) and media supplements (NEAA and NaPyr) used are from Lonza.

3.4 Immunoprecipitation (IP)

HeLa, HEK 293, JEG-3, Caco-2 and Cos-7 cells were harvested by scraping and lyzed for 30 min at 4 ºC in 20 mM Tris pH 7.5, 137 mM NaCl, 2 mM EDTA, 1 % NP-40 and complete mini-protease inhibitor mixture (Roche). Lysates were cleared by centrifugation (10 min, 10 000 g, 4 ºC) and the protein concentration was determined using Quick Start™ Bradford Protein Assay (Bio-Rad). Standard curve using Bovine Serum Albumine (BSA) was determined according to manufacturer's instructions as shown in Figure 7.

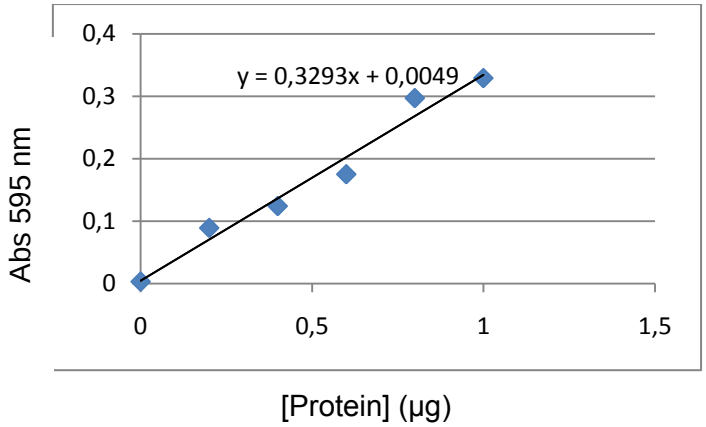

Figure 7 Standard curve obtained using Bovine Serum Albumine (BSA).

Lysates were pre-cleared for 30 min at 4 ºC with rotation with either Protein G sepharose resin (GE Healthcare) or Protein G magnetic beads (Millipore) and incubated overnight at 4 ºC with the antibody specific for the protein to be immunoprecipitated (optimized dilutions for each antibody are shown on Table 1) (Figure 8A). Before use Protein G sepharose resin was washed three times with phosphate buffered saline (PBS) and used in a 50 % slurry (50 % sepharose resin in PBS). Protein G magnetic beads were washed three times in 0.2 % Tween in PBS according to manufacturer's instructions.

Either one was then added to the lysates and incubated for 3 h, at 4 ºC with rotation (Figure 8B). Recovery of the immunocomplexes bound to the Protein G magnetic beads was done with the aid of a magnetic rack (Millipore) while recovery of the immunocomplexes bound to Protein G sepharose resin was done by centrifugation (Figure 8C).

Magnetic beads or sepharose resin were washed twice with 20 mM Tris pH 7.5, 137 mM NaCl, 2 mM EDTA, 0.1 % NP-40 and resuspended in Laemmli buffer (0.25 mM Tris pH 6.8, 8 % sodium dodecyl sulfate (SDS), 40 % glycerol, 10 % β-mercaptoethanol and 0.008 % of bromophenol blue). Samples were denatured at 95 ºC for 10 min and resolved using SDS–polyacrylamide gel electrophoresis (SDS–PAGE).

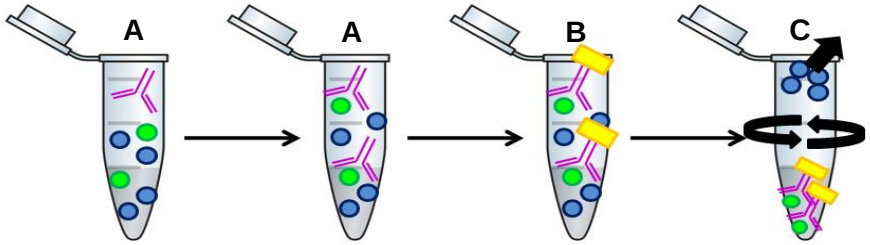

Figure 8 Schematic representation of the IP procedure. **(A)** Incubation of the cell lysates with the antibody specific for the protein to be precipitated. **(B)** Addition of the Protein G sepharose resin or Protein G magnetic beads. **(C)** Recovery of the immunocomplexes.

3.5 Sodium dodecyl sulfate-polyacrilamide gel electrophoresis

SDS-PAGE is a biochemical method that allows the separation of different proteins based on their electrophoretic mobility. SDS is an anionic detergent used as a denaturant to maintain the proteins in their linear state and to impart negative charge to the linear protein. This method allows the fractionation of the proteins by their approximate size.

Polyacrilamide gel is divided in two sections, a stacking and separating gel solutions. Stacking is meant to align all proteins so that they can start the electrophoretic run at

the same point and the separating solution to allow separation of the different molecules based on their size (Moser et al., 2009).

For all performed SDS-PAGE procedures throughout this work a 0.75 mm thick, 8 % (vol/vol) polyacrilamide gel was used.

Components and volumes used for stacking and 8 % resolving polyacrilamide gel solutions are described in Table 3.

Table 3 Components and volumes used to do a stacking and 8% resolving polyacrilamide gel.

RESOLVING GEL	Volumes
H_2O	2,6 ml
30 % Acrilamide/ Bis Solution	1 ml
Tris 1.5 M pH 8.8	1,3 ml
SDS 10 %	50 µl
APS 10 %	50 µl
Temed	4 µl
Total Volume	5 ml

STACKING GEL	Volumes
H_2O	1,24 ml
30 % Acrilamide/ Bis Solution	250 µl
Tris 0.5 M pH 6.8	500 µl
SDS 10 %	20 µl
APS 10 %	20 µl
Temed	2 µl
Total Volume	2 ml

The same buffer is used at the anode and cathode, Tris/Glycine/SDS Buffer (TGS 1x). An electric field (100V) is applied to the gel allowing the migration of the negatively charged molecules towards the positive electrode, the anode. Separation of the proteins occurs based on their molecular weight. Bigger sized molecules migrate slower in the gel while smaller sized molecules migrate faster (Moser et al., 2009).

3.6 Western Blot

Proteins are transblotted for 70 min at 0.25 mA, using Trans-Blot Turbo (Bio-Rad), from the polyaclilamide gel onto nitrocellulose membranes (Bio-Rad) (Figure 9). Efficiency of the transfer is ensured by the reversible stain of the membrane with Ponceau S (Sigma Aldrich) (Moser et al., 2009).

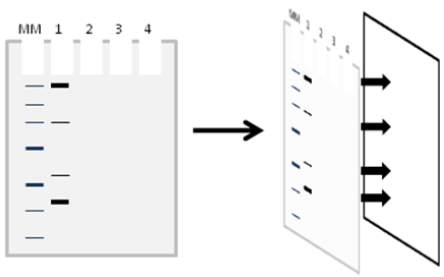

Figure 9 Schematic representation of the transfer procedure. Through use of a charged buffer proteins are transferred from the polyacrilamide gel onto a nitrocellulose membrane.

After transfer, membranes were blocked with 5 % skimmed milk for 2 h at room temperature, washed 5 min with 0.2 % Tween in PBS and, probed with an antibody against the protein of interest overnight at 4 ºC (optimized dilutions shown in Table 1).
The following day membranes were washed 3 times (10 min per wash) to eliminate the excess of primary antibody, in 0.2 % Tween in PBS and probed with the corresponding horseradish peroxidase-conjugated secondary antibody for 45 min at room temperature (RT). Three additional 10 min washes were done. Detection of proteins was performed by enhanced chemiluminescence (ECL) (Thermo Scientific or Bio-Rad) (Figure 10).

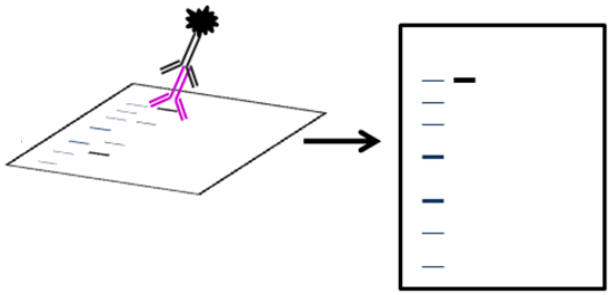

Figure 10 Schematic representation of the Western Blot procedure. Depicted in pink is the molecule corresponding to the primary antibody and in black the horseradish peroxidase-conjugated secondary antibody.

3.7 Transfection of HEK 293 and Cos-7 cells

The day before the transfection, HEK 293 and Cos-7 cells were seeded at the density of $2.5x10^5$ cells per well in a 6-well plate and $2x10^6$ cells per 10 cm plate.
Transfection of pGFP (C3), pGFPMIIB and pGFPMIIA (Table 2) in these cell lines is achieved following JetPRIME's (Polyplus^{TM}) recommended transfection protocol.
For optimization of GFP-tagged NMIIA expression in HEK 293 cells in a 6-well plate: 0.5, 1, 2 or 3 µg of pGFPMIIA were used for transfection.
For transfection of HEK 293 and Cos-7 cells seeded in 10 cm plates, 12 µg of pGFP (C3), pGFPMIIB or pGFPMIIA were used.
Briefly, 12 µg of DNA were mixed with 24 µl of JetPRIME Reagent (1:2 ratio). Transfection mix was incubated 10 min at RT and then added, drop by drop, to the plate.
Cells were incubated overnight at 37 ºC with appropriate regularly used cell culture media. 24 h post-transfection cells were harvested by scraping and the lysates used for IP assays.

3.8 Transfection of Caco-2 cells

Caco-2 cells were seeded at a density of $2x10^6$ cells per 10 cm plate the day before the transfection.

Transfection was done using Lipofectamine 2000 (Invitrogen) according to manufacturer's instructions. Caco-2 cells were transfected with 12 µg of pGFP (C3), pGFPMIIA or pGFPMIIA-Y158F (Table 2). Lipofectamine 2000 was diluted in Opti-MEM medium. DNA was diluted in Opti-MEM medium and added to the tube containing the diluted Lipofectamine 2000 in a 1:1 ratio. The transfection mix was incubated 5 min at RT and then added, drop by drop, to the plate. Cells were incubated at 37 ºC for 4 h and after that time period culture media was replaced.

The day after transfection cell culture media was changed to a selective media containing 1 mg/ml of geneticin (G148) to initiate selection of transfected cells. Cells were maintained in culture media with 0.7 mg/ml of G148 for approximately 2 weeks. Selective culture media was replaced every two days. Cells were collected and GFP-positive cells were sorted by flow cytometry and transferred to a 24-well plate and incubated with selective culture media. Cells were allowed to expand into a T75 flask and some aliquots were frozen for storage at -80 ºC.

3.9 Protocol for Freezing Caco-2 cells transiently expressing GFP, GFPMIIA and GFPMIIA-Y158

A confluent T75 flask was used to freeze two cryo-vials.

Culture media was removed and cells were washed twice with sterile PBS and 1ml of 0.25 % trypsin/EDTA (1x) (Gibco®) was added. Cells were incubated at 37 ºC for 5 min, 4 ml of culture media were added and cells were recovered by vigorous pipetting and transferred to a 15 ml Falcon tube.

Cells were centrifuged at 300 g for 5 min and resuspended in 2 ml of freezing media (Caco-2 selective culture media plus 10 % DMSO).

3.10 Seeding, maintenance and retrieval of cells in TRANSWELL filters

3.10.1 Seeding

Caco-2 cells were seeded at a density of $2x10^5$ cells per TRANSWELL filter (Corning) (Figure 11).

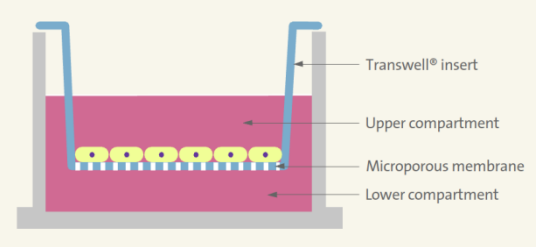

Figure 11 TRANSWELL Filter representation (Corning).

Before seeding Caco-2 cells were collected from a T75 flask and resuspended to obtain a single cell suspension.

Number of cells in 10 µl of cell suspension was determined using a cell counter (Invitrogen).

The required volume of cell suspension containing $2x10^5$ cells per filter was calculated. Calculated volume of cell suspension was transferred to a 15 ml falcon tube and centrifuged for 5 min at 300 g. Supernatant was discarded and 100 µl, of media, were added per filter to the obtained pellet of cells, e.g. for 6 filters add 600 µl of culture media. Cells were gently resuspended.

100 µl of the homogenized cell suspension were added to the upper compartment of each TRANSWELL filter already containing 100 µl of culture media. TRANSWELL filters must have 1 ml of media in the lower compartment and 200 µl in the upper compartment.

3.10.2 Maintenance

To change media on TRANSWELL filters 1 ml of culture media was added to an empty well in the plate containing the filters. The filter was picked up with forceps and held at a 45º angle to remove the old medium completely with a 200 µl tip. The tip should never touch the cell monolayer to avoid disruption. The empty filters were then placed in the wells with 1 ml of fresh culture media. The 200 µl of culture media to the upper compartment were added gently with the tip against the wall of the filter, to avoid disrupting the monolayer. The used medium in the wells was maintained there until the next media change as a quality control, to assure that there were no contaminants in the filters. Media was replaced twice a week.

3.10.3 Retrieval

To perform IF staining on polarized cells grown on TRANSWELL filters the initial steps on the staining process including fixation, quenching and blocking were done in the 24-well plate. All solutions were added at the appropriate volume to the filter (1 ml in the lower compartment and 200 µl in the upper compartment).
After the initial steps the filter was carefully detached from the bracket with the help of a scalpel and forceps. The remaining IF staining procedure is described in section 3.11.

3.11 Immunofluorescence (IF) microscopy

Caco-2 cells were seeded at a density of $2x10^5$ cells per TRANSWELL filter and allowed to polarize for 10 days. Cells were fixed in 3 % paraformaldehyde (PFA), 200 µl in the upper compartment of the filter and 1 ml in the lower compartment, for 20 min at RT and quenched for 90 min with 50 mM NH_4Cl. Permeabilization was achieved with 0.2 % saponin in PBS for 5 min. Saponin was included throughout all the washing and antibody solutions for the rest of the IF process. Blocking was done with 1 % BSA in PBS for 30 minutes at room temperature. TRANSWELL filters were incubated 1 h in a 20 µl solution with primary antibodies and washed three times in 0.2 % saponin in PBS. Filters were incubated with secondary antibodies and Phalloidin-647 for 45 min at RT in the dark. DNA was counterstained with DAPI (Sigma-Aldrich).
Filters were washed once in 0.2 % saponin in PBS, once in PBS and a third time in distillated H_2O before being mounted in glass slides with 5 µl of Aqua-Poly/Mount (Polysciences). Images were acquired with an Olympus BX53 microscope using the 40x or 60x objectives.

4. Results

4.1 Results from the yeast two-hybrid screen

This assay allowed the analysis of 232 million interactions of which 97 were positive and validated by HYBRIGENICS.

The detected interactions are also scored according to a global Predicted Biological Score (PBS®) that is used to assess the reliability of the interaction.

The predicted biological score integrates local and global information. Local information refers only to our screen, while global information results from the integration of information from all screenings by HYBRIGENICS in a placental library. Integration of global information permits the identification of proteins that retrieve identical partners in different screens (HYBRIGENICS and Rain et al., 2001).

PBS® ranges from A to F. Ratings A, B, C and D represent very high, high, good and moderate confidence interactions, respectively. D rated interactions are usually identified through one unique prey fragment (just one hit in the Y2H) or multiple identical ones. Interactions labeled with D can also correspond to interactions that are weakly detected in the Y2H system. Weak detection can occur because: of low representation of mRNA of the prey protein in the selected library; specific folding of the prey protein, which will inhibit binding to the bait protein; in the yeast system the prey protein cannot be modified post-translationally and doesn't acquire the conformation required to bind our bait protein or possible toxicity provocked by the prey protein in yeast cells. Interactions labeled with D might also mark false-positive interactions. Interactions rated with E encompass conserved prey proteins that are known to bind unspecific sequences in a variety of target proteins and F corresponds to experimentally proven technical artifacts.

The regions of the prey proteins that interact with our bait protein were characterized by several features including: the reading frame; if the coding region of the prey is complete; if the fragment is localized at the 5' or 3' untranslated regions and if it contains STOP codons in the reading frame.

4.2 Selection of the Target-Proteins

From the 97 positive and validated interactions in the Y2H screen, five were selected for further studies including their molecular characterization and the role of their

interaction with NMIIA. Our aim is to increase our knowledge about NMIIA starting with its interacting partners.

In Table 4 are represented the five selected target proteins. They were: ZNF12, SMPD4, AFF1, β-adaptin and Hsp56. The domains of the prey proteins identified to interact with the tail of NMIIA are indicated in Figure 12.

Table 4 Target proteins selected from the Y2H screening. Five selected targets are described in the table along with their obtained PBS®. Localization of the interaction domain with the bait protein is presented for the nucleotide and amino acid sequences. All selected targets were in frame (IF). Last column represents the number of hits each target had in the Y2H assay.

Target Protein Name	PBS®	Interaction domain (nt)	Interaction domain (aa)	Frame	Number of Hits
ZNF12	A	33-2891	422-597	IF	23
SMPD4	B	57-745	33-243	IF	4
AFF1	C	2331-3143	872-1046	IF	2
β-Adaptin	D	711-1430	238-476	IF	1
Hsp56	D	57-1150	20-383	IF	1

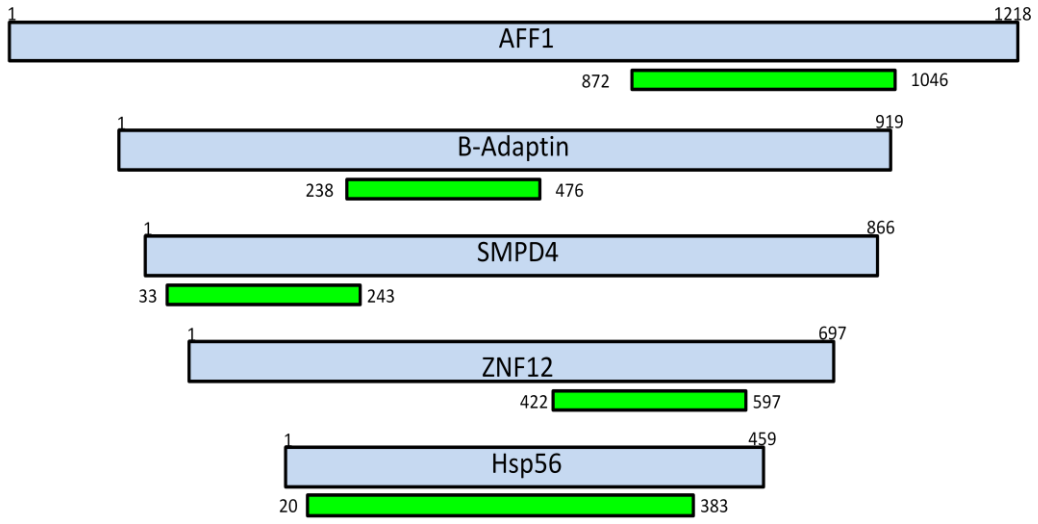

Figure 12 Schematic representation of the Selected Interaction Domain (SID) of the selected prey proteins. Amino acid sequences of the five selected targets are depicted in blue and domain of the prey protein that interacted with the bait fragment in Y2H assay is depicted in green.

4.2.1 Zinc-Finger Protein 12 (ZNF12)

Zinc-finger (ZNF) domains have multiple functions such as DNA-binding (transcriptional regulation), protein-protein interactions, RNA-binding and membrane association (Laity et al., 2001; Mackay and Crossley, 1998). Zinc-fingers are considered small, functional

domains that require coordination of zinc ions to stabilize their structure (Laity et al., 2001).

ZNF12 was identified as a NMIIA binding partner in the Y2H with a PBS of A (very high confidence in the interaction). It belongs to the Krüppel Cys_2His_2 zinc-finger (ZNF) protein family, designated as the classical ZNF family. ZNF12 contains eight Cys_2His_2-type zinc fingers and a Krüppel associated box (KRAB) domain that functions as a transcriptional repressor. This protein family is involved in DNA transcription and mediating protein-protein interactions with direct influence on gene expression (Gamsjaeger et al., 2006).

ZNFs are poorly studied and commonly reported as mediators of protein-protein interactions and are described as “sticky” because of their affinity to bind various proteins through interaction of a single ZNF domain (Mackay and Crossley, 1998). Translocation of transcription factors to the nucleus is usually aided by motor proteins.

4.2.2 AF4/FMR2 Family Member 1 (AFF1)

The AF4/FMR2 protein family is composed of proteins that act as transcriptional activators that are also involved in the RNA elongation process and chromatin remodeling. AFF1 is described as being localized in the nucleus, same as the remaining members of the AF4/FMR2 family proteins, where it appears with a diffused appearance in small clusters (Spector and Lamond, 2011). This protein family has a common domain organization with an N and C terminal homology domains, a highly conserved serine-rich transactivation domain (TAD) and an AF4/LAF4/FMR2 (ALF) homology domain. Functions of the N and the C terminal domains are not known and ALF was recently described to be involved in proteosomal degradation pathways (Bitoun et al., 2006). AFF1 was rated C and was identified twice in the Y2H. This protein is described to be expressed ubiquitously but with increased expression on the lymphatic system and the placenta.

4.2.3 Sphingomyelin phosphodiesterase 4 (SMPD4)

SMPD4 catalyzes the hydrolysis of membrane sphingomyelin to form phosphorylcholine and ceramide. Inside the cell this protein is usually membrane bound, being found in the endoplasmic reticulum membrane and on the Golgi apparatus membrane. Ceramide can serve as both a structural and a signaling molecule and has been implicated in processes such as: cell cycle arrest, apoptosis,

inflammation and eukaryotic stress response (Corcoran et al., 2008). SMPD4 was selected based on its PBS® and the 4 obtained hits in the Y2H.

4.2.4 Beta-adaptin (β-adaptin), subunit of the adaptor protein complex 1

Adaptor protein (AP) complexes are constituted by subunits designated adaptins. Each complex has four subunits: two large subunits (γ/α/δ/ε and β1 to β4, belonging from AP1 to AP4, respectively), one medium subunit (μ1 to μ4) and one small subunit (σ1 to σ4) (Figure 13).

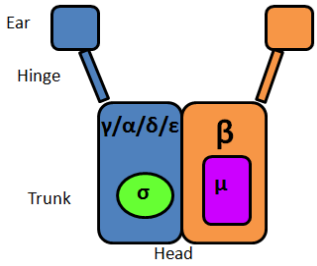

Figure 13 Schematic representation of an AP complex. Different subunits are depicted in different colors.

To date four AP complexes have been described: AP1, AP2, AP3 and AP4. Clathrin-coated vesicles (CCV) that travel the endocytic and secretory pathways usually have a protein coat on their cytoplasmic face that among its components contains the AP complexes. Besides forming the protein coat these complexes are also responsible for the selection of the cargo the vesicle is going to transport (Boehm and Bonifacino, 2001). AP2 acts specifically at the plasma membrane in endocytic processes while AP1, AP3 and potencially AP4 are associated with the formation of clathrin-coated vesicles from intracellular membranes (McMahon and Boucrot, 2011).

Beta-adaptin (β-adaptin), a subunit of the adaptor protein complex 1 (AP1) is commonly found inside the cell on the cytoplasmic face of the CCV located at the Golgi complex, where it mediates the recruitment of clathrin and the recognition of sorting signals located on the cytosolic tails of transmembrane cargo molecules. Adaptor complexes are capable of recognizing and binding both tyrosine-based and dileucine-based sorting signals through the recognition of different sequences specific to each sorting motif (Carvajal-Gonzalez et al., 2012; Rapoport et al., 1998). Tyrosine-based sorting signals have the consensus sequence YXXφ, where X is any amino acid and φ is a hydrophobic amino acid whereas dileucine-based sorting motifs usually bind to the consensus sequence [DE]XXXL[LI] (Rapoport et al., 1997; Rapoport et al., 1998; Carvajal-Gonzalez et al., 2012; Ihrke et al., 2004). The AP1 complex is involved in the basolateral recycling of Coxsackie-adenovirus receptor (CAR) after its internalization (Diaz et al., 2009). CAR possesses a commom tyrosine-sorting motif (YXXφ) that is recognized by the medium subunit (μ1) of the AP1 complex. β-adaptin binds dileucine-sorting motifs (Rapoport et al., 1998). It has yet to be described if the two subunits can bind the same molecule at the same time.

AP1 has been proved important to bacterial and viral infections. AP1 may localize at the plasma membrane when large cargoes need to be internalized by the cell. This protein is thought to form a flat array at the entry site and act as a signaling molecule to begin actin polymerization. AP1 is required for *L. monocytogenes* entry into host cells (McMahon and Boucrot, 2011; Pizarro-Cerdá et al., 2007). Our group has recently reported the relocation of NMIIA to the interface of *L. monocytogenes* with the host cell membrane (Almeida et al., submitted). Despite its D rating β-adaptin was selected based in its cellular functions and previously documented involvement in *L. monocytogenes* infection.

4.2.5 Heat-shock protein 56 (Hsp56)

The second NMIIA interacting partner rated with D was Hsp56. This protein is considered a high molecular weight immunophilin and it was identified for the first time associated with steroid hormone receptors. It is involved in immunoregulation and basic cellular processes involving protein folding and intracellular trafficking. This protein is a known target of the immunosuppressive drug FK506 and this property assigned it to a subclass of immunophilins designated FK506-binding proteins (FKBPs) It is composed of an N-terminal peptidylprolyl *cis-trans* isomerase (PPIase) domain and a C-terminal tetratricopeptide repeat (TPR) domain which is responsible for mediating protein-protein interactions (Scammell et al., 2003 and Davies and Sánchez, 2005).
This protein is capable of modulating microtubule function (Cioffi et al., 2011; Chambraud et al., 2010).
Hsp56 is known to associate with two heat shock proteins (hsp90 and hsp70) and play a role in intracellular trafficking of hetero-oligomeric forms of steroid hormone receptors between the cytoplasmic and nuclear compartments. To this purpose Hsp56 binds dynein. The binding with dynein allows the translocation of the hormone complex from the cytoplasm to the nucleus (Davies and Sánchez, 2005; Sivils et al., 2011). Furthermore Hsp90 is a Gp96 paralogue, both originated from the same ancestral gene but are now localized at distinct sites in the genome. This protein was identified as a surface receptor for a *L. monocytogenes* virulence factor, Vip. The interaction is required for bacterial entry into host cells (Cabanes et al., 2005; Martins et al., 2012).

4.3 Expression levels of the five selected targets in HeLa, HEK 293 and Jeg-3 cell lines

ZNF12 is a nuclear protein that presents similar expression levels in kidney, cervical and placental tissues. SMPD4 is preferentially localized at the ER membrane, data regarding expression levels of the protein showed high expression levels in the lymphatic system and low expression levels in kidney tissue. AFF1 is a transcriptional activator highly expressed in the placenta. Hsp56 is mainly cytoplasmic and presents very equivalent expression levels throughout all the major tissues. β-adaptin can be localized at the Golgi complex or throughout the cytoplasm in the clathrin coat of CCVs. This protein is highly expressed in the nervous system as well as in the placenta. Expression data described here was acquired from the GeneCards database.

We first analyze the expression levels of each target protein in HeLa, HEK 293 and Jeg-3 cell lines by immunoblot with antibodies specific for each protein. Cells from each cell line were harvested, lyzed and the total protein quantified and 20 µg of total protein used for western blot (WB) analysis.

AFF1 has a predicted molecular weight 131 kDa. Immunoblot with an antibody against AFF1 revealed a very faint band, in all 3 cell lines, with a molecular weight below 100 kDa (Figure 14A). Immunoblot against Hsp56 revealed a single band with the predicted molecular weight of 59 kDa in HeLa and HEK 293 cells. In Jeg-3 cells two bands were detected, the major band corresponding to Hsp56 (Figure 14B). In Figure 14C detection of β-adaptin revealed a band over 100 kDa in all cell lines, corresponding to predicted molecular weight of 106 kDa. SMPD4 has a predicted molecular weight of 93 kDa, however we could not detect any signal in the blot (Figure 14D). In Figure 14E, the antibody anti-ZNF12 detected several bands with different molecular weights. ZNF12 seems to correspond to the most intense band. In summary, the antibody against AFF1 faintly detected a band lower than the predicted molecular weight and SMPD4 could not be detected by immunoblot in any of the used cell lines. Antibody against ZNF12 recognized several bands, but produced a more intense band corresponding to the target-protein. Antibodies against Hsp56 and β-adaptin detected the proteins with the predicted molecular weight in all three cell lines.

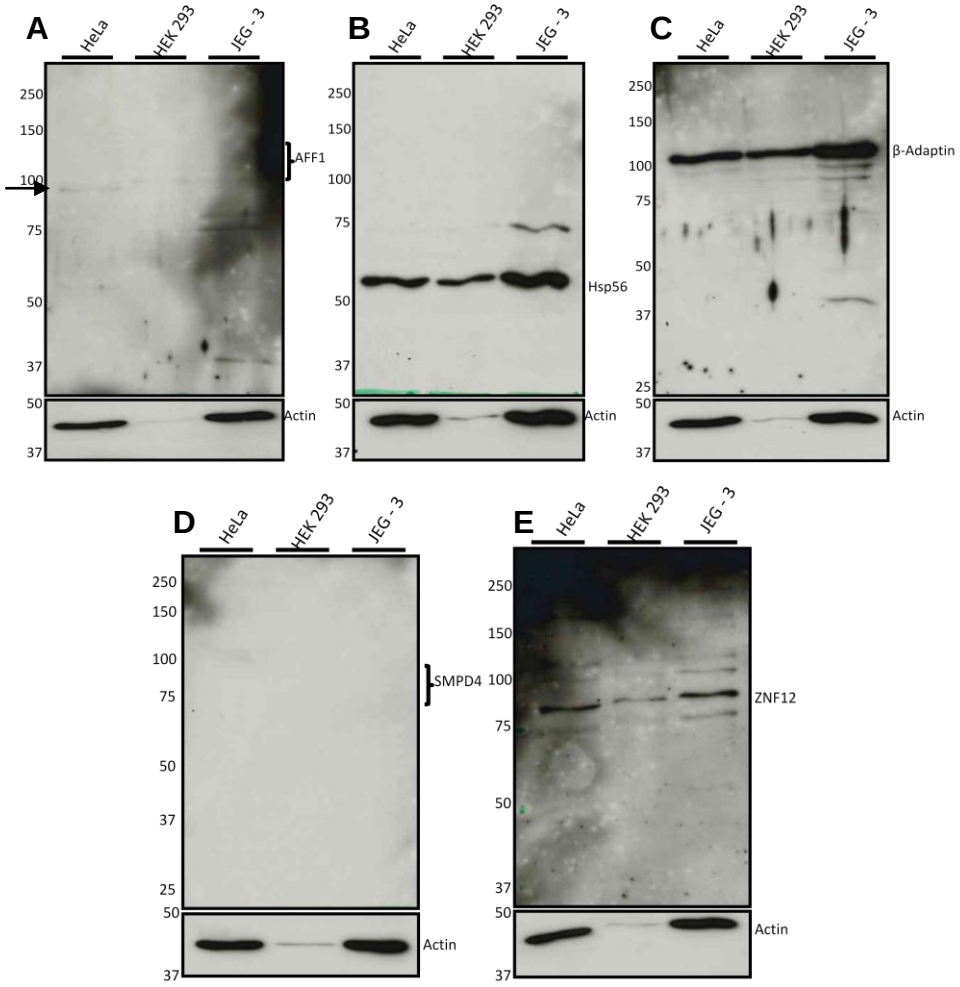

Figure 14 Expression levels of AFF1 **(A)**, Hsp56 **(B)**, β-Adaptin **(C),** SMPD4 **(D)** and ZNF12 **(E)** in HeLa, HEK 293 and Jeg-3 cell lines. For each cell line 20 µg of total protein were used for WB analysis. Detection of actin protein levels was used as loading control.

4.4 Optimization of the immunoprecipitation of NMIIA

To biochemically confirm the results obtained in the Y2H assay we performed immunoprecipitation assays (IPs). This method consists in precipitating a selected protein, using a specific antibody, from a whole cell lysate and this way retrieve its interacting partners (Dwane and Kiely, 2011).

Two different IPs were optimized to serve as platforms to be used in the confirmation of the interactions: the IP of endogenous NMIIA and the IP of ectopically expressed GFP-tagged NMIIA, in which the protein is overexpressed in cells.

The first task was to optimize the IP of endogenous NMIIA from HeLa and Jeg-3 cell lysates.

HeLa cells were harvested and lysed and protein concentration was determined. To ascertain which amount of antibody would immunoprecipitate NMIIA more efficiently three antibody to total protein ratios were tested (1:500, 1:100 and 1:50).

NMIIA was immunoprecipitated from 100 µg of total protein by adding 0.2, 1 or 2 µg of anti-NMIIA polyclonal antibody (Sigma Aldrich) and 50 µl of a Protein G sepharose resin slurry (50 % sepharose resin in PBS). Immunocomplexes were recovered and resolved by SDS-PAGE. Detection of NMIIA was done by immunoblot.

IP of NMIIA using 0.2 µg of antibody produced no enrichment when compared to the INPUT. When 1 or 2 µg of antibody were used to immunoprecipitate NMIIA there was an enrichment of NMIIA in the IP fraction when compared to the INPUT. The 1:100 ratio was thus selected to standard use in the IP of NMIIA. The flow-through (FT) was used as a control to check the amount of NMIIA that was not immunoprecipitated (Figure 15A).

NMIIA was immunoprecipitated from 500 µg of total protein by adding 5 µg of anti-NMIIA polyclonal antibody (1:100 ratio) and 50 µl of a Protein G sepharose resin 50 % slurry. Two control conditions were used: cell lysates incubated only with protein G sepharose resin (Figure 15B) and lysates incubated with an isotype control antibody and Protein G sepharose resin (Figure 15C). Some unspecific binding to the control was detected in Figure 15B. No NMIIA was present in the control lane in Figure 15C.

In this experimental conditions we successfully immunoprecipitated NMIIA (Figure 15B and 15C).

NMIIA was also immunoprecipitated from 300 µg of total protein from Jeg-3 cell lysates. As a control cells were incubated with an isotype control antibody and Protein G sepharose resin. No NMIIA appeared associated with the isotype control antibody. NMIIA was enriched in the IP fraction when compared to the INPUT (Figure 15D). Actin was used as a loading control (Figure 15A, 15B, 15C and 15D).

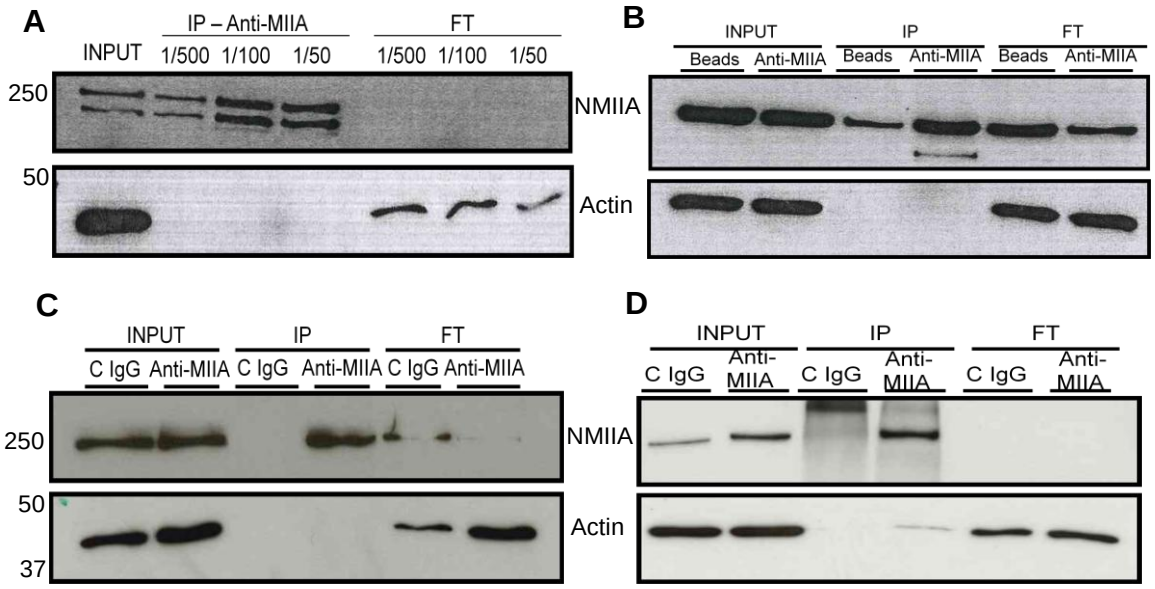

Figure 15 IP of endogenous NMIIA in HeLa **(A, B and C)** and Jeg-3 **(D)** cells. Optimization experiment was performed with 100 µg of protein and 3 antibody to total protein ratios. Scale-up experiments were performed with 500 µg of protein in HeLa cells and 300 µg in Jeg-3 cells. A 1 to 100 antibody to total protein ratio was used. Detection of actin protein levels was used as loading control. **(A)** Optimization of the IP of endogenous NMIIA. **(B)** Scale-up IP of endogenous NMIIA. Whole cell lysates were incubated with protein G sepharose resin as a control condition. **(C)** Scale-up IP of endogenous NMIIA. Lysates were incubated with an isotype control antibody and protein G sepharose resin as control. **(D)** Scale-up IP of endogenous NMIIA in Jeg-3 cells.

Optimization of the ectopic expression of GFP-tagged NMIIA (GFP-NMIIA) was performed in 6-well plates and asserted by flow cytometry and IF.

HEK 293 cells were transfected with increasing amounts of a plasmid enconding GFP-NMIIA (Table 5). Mock transfected cells (incubated with the transfection reagent but no DNA) were used as control. Selection of GFP-positive cells was performed by flow cytometry. Where a fluorescence threshold is determined and only cells with GFP fluorescence above the threshold are sorted as GFP-positive.

Mock transfected cells had 2.57 % of GFP-positive cells, probably due to self-fluorescence. Cells transfected with 2 µg of pGFPMIIA, showed 56 % of GFP-positive cells. In the remaining conditions percentage of GFP-positive cells was always inferior, ranging from 12.2 % to 38.7 % (Figure 16A and Table 5).

To confirm the results obtained by flow cytometry we performed immunofluorescence. HEK 293 cells expressing GFP-NMIIA were stained for DNA (DAPI). HEK 293 cells transfected with 2 µg of pGFPMIIA displayed the higher number of GFP-positive cells, as shown by flow cytometry (Figure 16B). To test the interactions transfection was scaled-up to a 10 cm plate. Amount of DNA used was determined according to the

area of the plates. Untrasfected cells were used as control. Transfection with 12 µg of DNA showed 44.7 % GFP-positive cells (Figure 16C).

Table 5 Results obtained by flow cytometry analysis of the optimization of the transfection of pGFPMIIA in HEK 293 cells. Amount of DNA used in each condition is indicated. Total number of sorted cells, number and percentage of GFP-positive and GFP-negative cells for each condition is shown in the table.

µg of pGFPMIIA	Total Cells	No. GFP(+)	No GFP(-)	%GFP(+)	%GFP(-)
Mock (0)	19509	502	19007	2.57	97.4
0.5	19156	2337	16819	12.2	87.8
1	11823	4319	7504	36.5	63.5
2	17957	10059	7898	56	44
3	22402	8662	13740	38.7	61.3

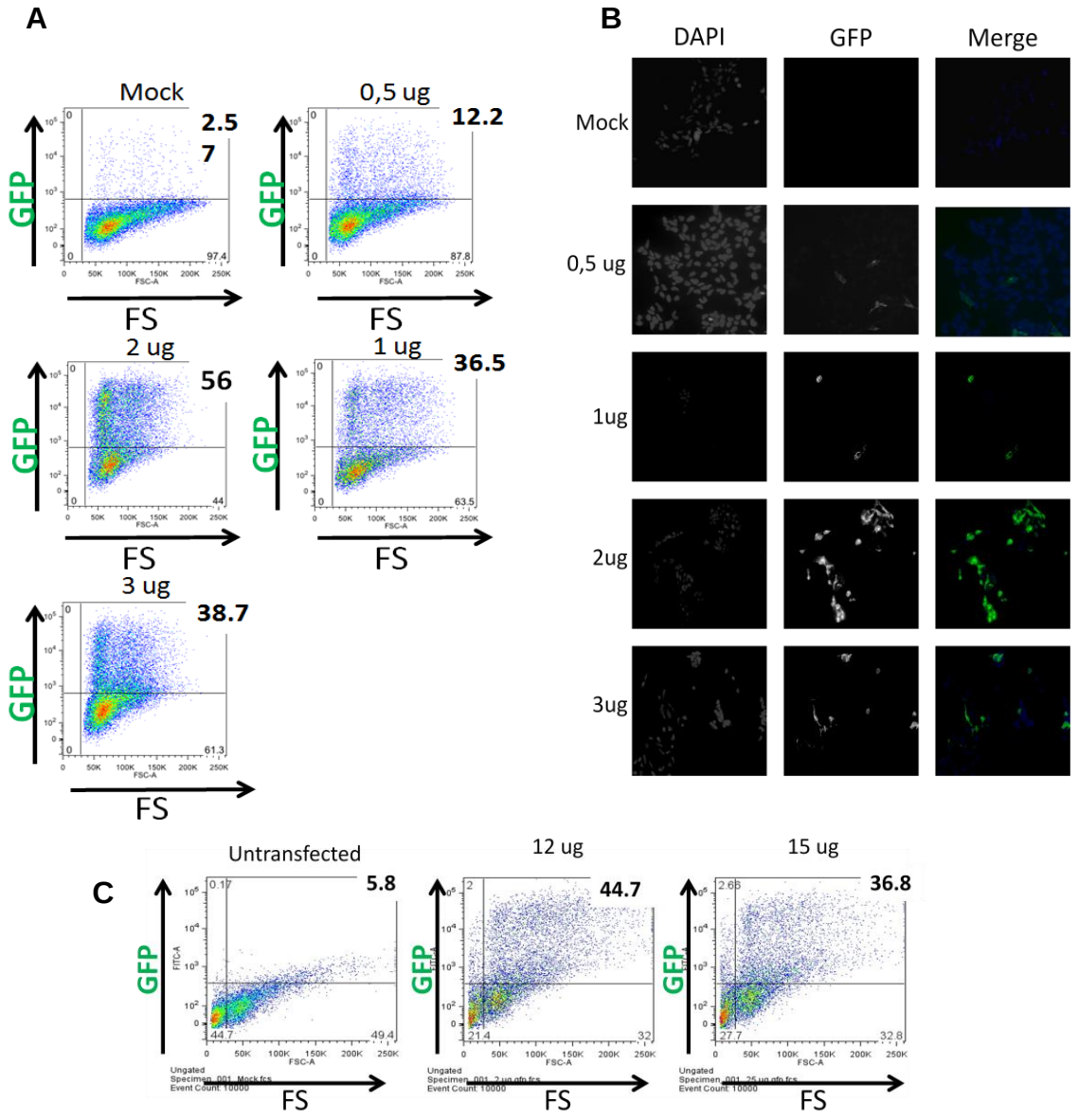

Figure 16 Optimization of the expression levels of GFP-tagged NMIIA in HEK 293. **(A)** Flow cytometry results from transfection on 6-well plates with increasing amounts of DNA **(B)** IF analysis of the expression of GFP-tagged NMIIA in each tested condition. **(C)** Flow cytometry analysis of transfection efficiency in 10 cm plates.

To test the interactions of NMIIA with the Y2H selected targets we transfected HEK 293 cells. Transfection was performed in 10 cm plates, lysates were recovered and protein concentration determined. GFP was immunoprecipitated from 100 µg of total protein by adding 20, 25 or 30 µl of agarose-conjugated anti-GFP (500 µg/ml). Immunocomplexes were recovered and samples were resolved by SDS-PAGE and immunoblotted with anti-GFP. Expression levels of GFP and GFP-tagged NMIIA were similar when analyzed by immunoblot (Figure 17A). However, analysis by IF showed a higher percentage of GFP-positive cells when cells were expressing only GFP (Figure 17B). IP of GFP alone was efficient and produced similar results with each amount of agarose-conjugated antibody used. IP of GFP-tagged NMIIA only occured when 20 or 25 µl of agarose-conjugated anti-GFP were used. However no enrichment was detected in the IP fraction in comparison with the INPUT (Figure 17A).
Given these results we thus performed IP of endogenous NMIIA to start confirming the interactions.

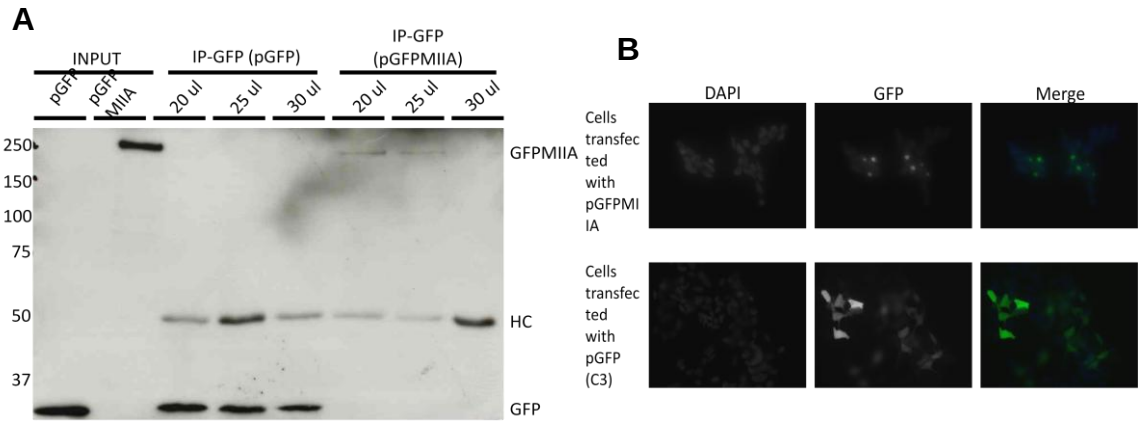

Figure 17 IP of ectopically expressed NMIIA in HEK 293 cells. **(A)** Optimization of the IP-GFP using increasing volumes of agarose-conjugated anti-GFP. **(B)** IF analysis of GFP-tagged NMIIA expression levels in HEK 293 cells transfected with pGFP or pGFPMIIA. DNA was counterstained with DAPI.

4.5 Evaluation of the interaction between NMIIA and ZNF12, SMPD4 and AFF1

To validate the interactions of NMIIA with Y2H selected targets HeLa cells were harvested, lysed and protein concentration measured. NMIIA was immunoprecipitated as described in section 4.4. As control, whole cell lysates were incubated with an isotype control antibody and protein G sepharose resin. No NMIIA associated with the

isotype control antibody. Detection of the target proteins was done by immunoblot with antibodies specific for each protein.

Anti-AFF1 did not detect any signal on the INPUTs. A very faint band was detected when 20 µg of protein were used (Figure 14A), not surprisingly the protein was not detected in less than 20 µg present in the INPUT. Thus it was not possible to determine if AFF1 associated with NMIIA (Figure 18a).

ZNF12 was weakly detected in the INPUTs but it was never detected in the IP fraction. This biochemical data does not allow the confirmation the interaction between this protein and NMIIA in these experimental conditions (Figure18b).

SMPD4 was faintly detected approximately at 100 kDa in the INPUT. This band was never detected in the IP fraction, suggesting that this protein does not co-IP with NMIIA (Figure 18c). This result does not allow the confirmation of the positive result obtained in the Y2H assay.

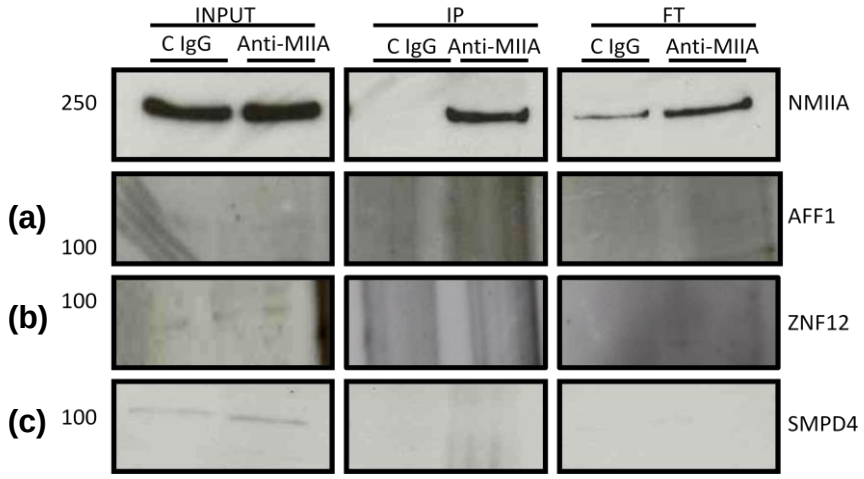

Figure 18 Evaluation of the interaction of NMIIA with AFF1 **(a)**, ZNF12 **(b)** and SMPD4 **(c)** by IP. **(a)** The antibody against AFF1 does not detect any signal. **(b)** ZNF12 was detected in INPUTs but not in the IP fraction. **(c)** A band with a different molecular weight from the one predicted for SMPD4 was detected in the INPUTs, but it wasn't detected in the IP fraction.

4.6 Evaluation of the interactions between NMIIA and β-adaptin and NMIIA and Hsp56

The interaction of two targets, Hsp56 and β-adaptin, with NMIIA remained to be evaluated. To confirm these interactions we proceeded as described.

In Figure 19A and 19B NMIIA was immunoprecipitated from 500 µg or 600 µg of protein from HeLa cell lysates, respectively, using the anti-NMIIA polyclonal antibody. Immunocomplexes were resolved by SDS-PAGE and immunoblotted with anti-β-adaptin and anti-Hsp56. Presence of β-adaptin associated with NMIIA was a

reproducible result. In 6 out of 9 experiments β-adaptin was associated with NMIIA, thus validating the Y2H screen data (Figure 19A and 19B). Hsp56 also appeared to co-IP with NMIIA in the majority of the performed experiments (Figure 19A and 19B). Together these results validate the data from Y2H indicating the direct binding between NMIIA and Hsp56 and β-adaptin.

Detection of actin protein levels in Figure 20B suggests different levels of protein between the two samples. Nevertheless the both targets appeared in the IP fraction associated with NMIIA (Figure 19B).

In some experiments: NMIIA associated with the isotype control antibody (Figure 20A), β-adaptin associated with the isotype control antibody (Figure 20B) and Hsp56 did not appear associated with NMIIA (Figure 20C).

However, considering all the experiments performed we overall consider that NMIIA interacts with both proteins and thus we focused the rest of the work performed in this project on these two targets.

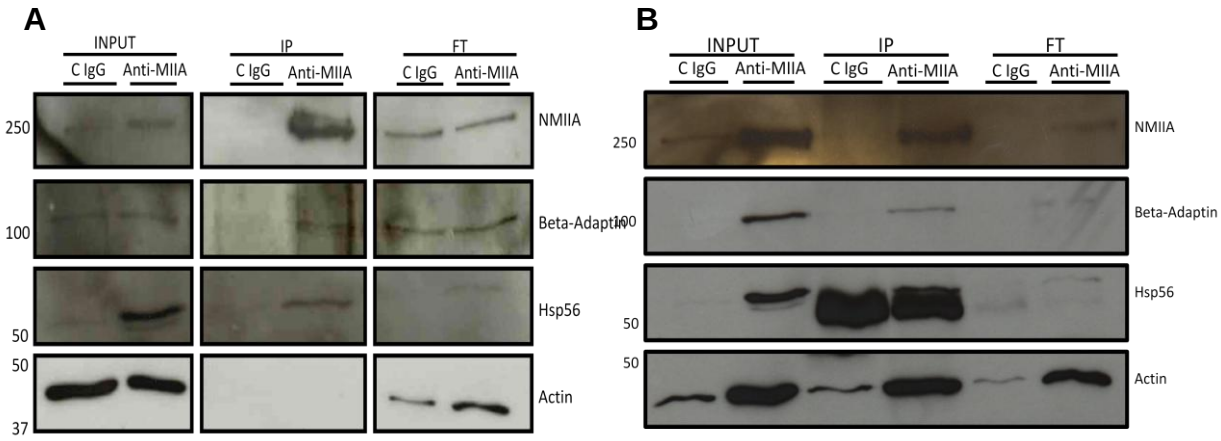

Figure 19 Evaluation of the interaction between: NMIIA and Hsp56 and NMIIA and β-adaptin. Detection of actin protein levels was used as loading control. **(A)** NMIIA was immunoprecipitated from 500 µg. β-adaptin and Hsp56 associated with NMIIA. **(B)** NMIIA was immunoprecipitated from 600 µg β-adaptin and Hsp56 also seem to co-IP with NMIIA.

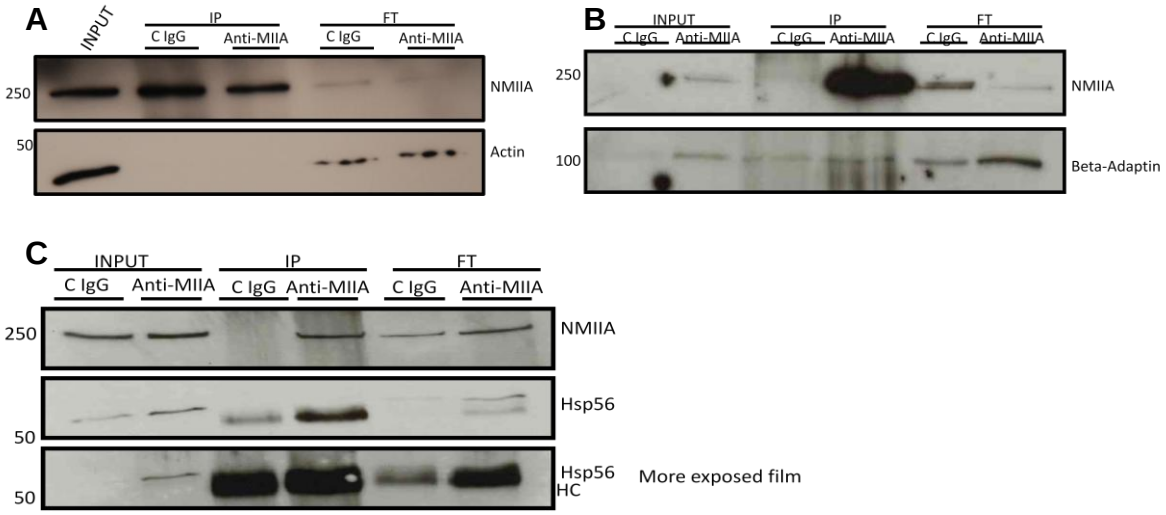

Figure 20 IP of endogenous NMIIA where detection of the interactions did not occur. Detection of actin protein levels was used as loading control. **(A)** NMIIA was successfully immunoprecipitated but appeared associated with the isotype control antibody. **(B)** IP of NMIIA was successful but β-adaptin appeared associated with the isotype control antibody. **(C)** IP of NMIIA was efficient but Hsp56 was not detected by immunoblot in the IP fraction.

4.7 Immunoprecipitation of Hsp56 and β-adaptin

To strengthen our results and prove the interactions we performed the reverse IP assays. We IP Hsp56 or β-adaptin and test for the presence of MIIA in the IP fractions by immunoblot.

For the optimization IPs of Hsp56 and β-adaptin: HeLa cells were harvested, lysed and protein concentration was determined. To determine which amount of antibody would be more efficient at immunoprecipitating the two proteins three antibody to total protein ratios were tested (1:500, 1:100 and 1:50).

Both target proteins were immunoprecipitated from 100 µg of total protein by adding 0.2, 1 or 2 µg of the specific antibody and 50 µl of Protein G magnetic beads. Immunocomplexes were recovered through the use of a magnetic rack (Millipore) and detection of the protein was done by immunoblot. Using 0.2 µg of antibody IP of Hsp56 (Figure 21A) and β-adaptin (Figure 21B) was efficient, but with small enrichment of these proteins in the IP fraction when compared to the INPUT. The 2 remaining conditions produced a significant enrichment of these proteins in the IP fraction in comparison with the INPUT and immunoprecipitated similar amounts of Hsp56 and β-adaptin. Thus the 1:100 ratio was selected as standard for all the next experiments. Membrane from the optimization experiments was probed with an antibody against

NMIIA. It was possible to observe an association between Hsp56 and NMIIA in the 1:100 ratio (Figure 21A) but it was difficult to detect the association with β-adaptin (Figure 21B).

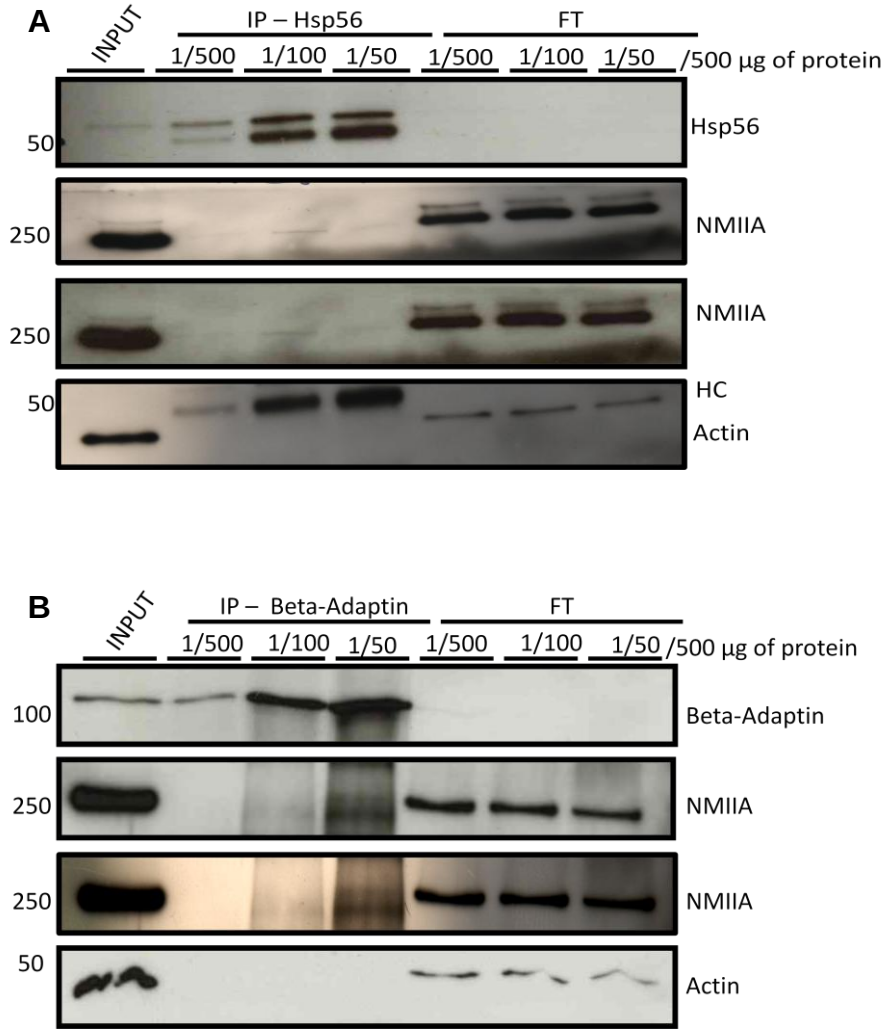

Figure 21 Optimization of the IP of Hsp56 and β-adaptin. Three antibody to total protein ratios were tested Detection of actin protein levels was used as loading control. **(A)** NMIIA seems to co-IP with Hsp56 in the 1:100 ratio condition. **(B)** Detection of NMIIA is difficult in the 1:50 ratio.

Scale-up IPs were performed for Hsp56 and β-adaptin using 300 and 500 µg of total protein, respectively, with the optimized 1:100 ratio. As controls: an antibody against the c-Myc tag (IP of Hsp56) and an isotype control antibody (IP of β-adaptin) were used. IP of Hsp56 (Figure 22A) was less efficient than the IP of β-adaptin (Figure 22B). Detection of NMIIA was performed by immunoblot. In Figure 22A very faint band corresponding to NMIIA appeared in the lane of the IP fraction. In Figure 22B NMIIA is

present in the IP fraction associated with β-adaptin. These results suggest an association between Hsp56 and β-adaptin and NMIIA thus confirming the results obtained in the Y2H.

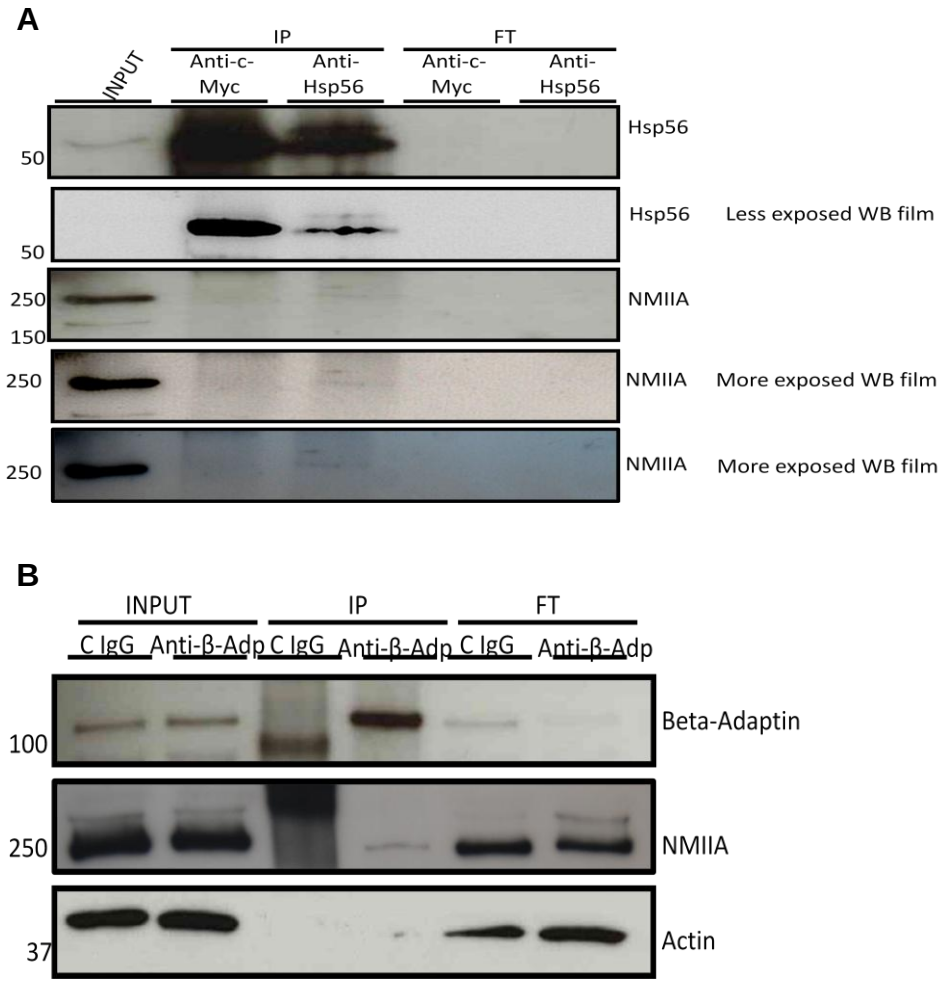

Figure 22 Scale-up IP of Hsp56 **(A)** and β-adaptin **(B).** Detection of actin protein levels was used as loading control. **(A)** Scale-up IP of Hsp56. A faint band corresponding to NMIIA is present in the IP fraction. **(B)** Scale-up IP of β-adaptin. NMIIA associates with β-adaptin in the IP fraction.

Additionally to the IP of β-adaptin in HeLa cells this protein was also IP in Cos-7 cells expressing GFP-NMIIA. Cos-7 cells do not express endogenous NMIIA. Expression levels of both our target proteins in Cos-7 cells were determined by western blot (Figure 23).

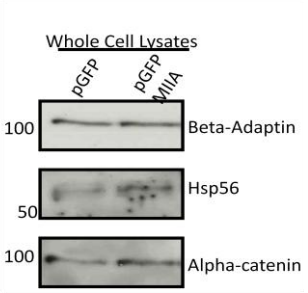

Figure 23 Expression levels of Hsp56 and β-adaptin in Cos-7 cells. Detection of the target proteins was done by immunoblot using an antibody specific for each protein. Alpha-catenin protein levels was used as loading control.

Cos-7 cells expressing GFP-NMIIA, GFP-NMIIB and GFP were used for the IP of β-adaptin. In all three experiments GFP-NMIIA always co-IP with β-adaptin (Figure 24A, 24B and 24C). In one of the three experiments a faint band corresponding to GFP can be detected associated with β-adaptin (Figure 24B). Biochemical data suggests that ectopically expressed GFP-NMIIA co-immunoprecipitates with β-adaptin in Cos-7 cells.
In summary, biochemical data from this chapter allows us to confirm the interactions detected in the Y2H between NMIIA and Hsp56 and NMIIA and β-adaptin.

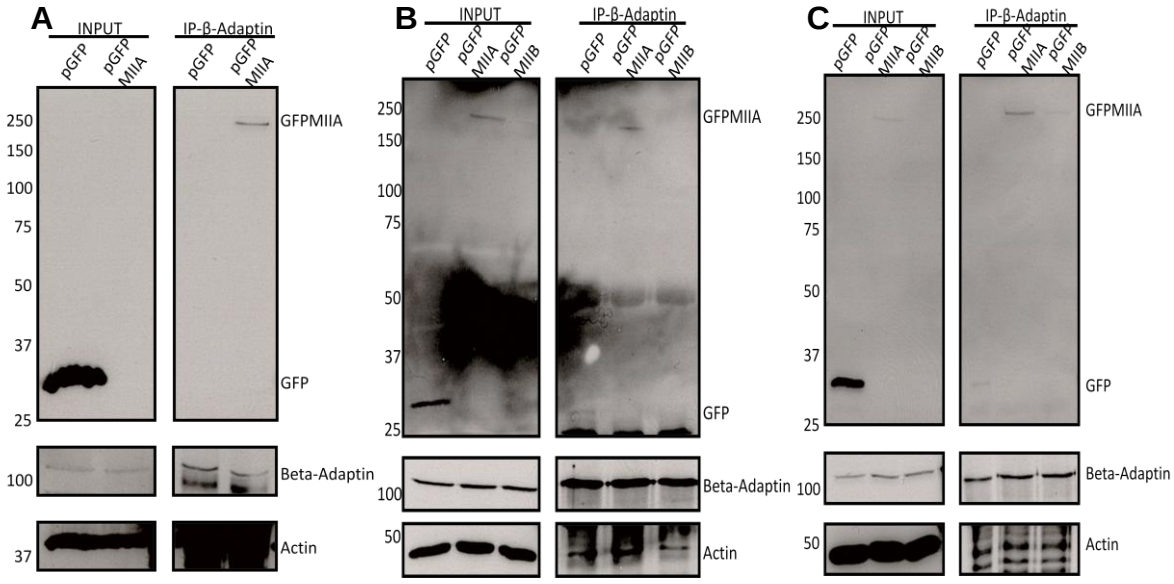

Figure 24 IP of β-adaptin in Cos-7. IP was performed in cells expressing GFP, GFP-NMIIA **(A)** or GFP-NMIIB **(B and C).** GFP NMIIA associated with β-adaptin in the three experiments. Detection of actin protein levels was used as loading control.

4.8 Non-muscle myosin IIA heavy chain bioinformatic sequence analysis

Sorting of cargo transported in clathrin-coated vesicles (CCVs) is regulated by the binding of adaptor protein (AP) complexes to sorting motifs present in the cargo proteins (Boehm and Bonifacino, 2001).
Adaptor protein complex 1 (AP1) is constituted by 4 subunits (Boehm and Bonifacino, 2001), two of them are described as binding tyrosine and dileucine sorting motifs in proteins to be sorted inside the cell (Rapoport et al., 1997, Rapoport et al., 1998; Carvajal-Gonzalez et al., 2012; Ihrke et al., 2004). The binding of the AP complexes is

regulated by phosphorylation of both the complex subunits and the cargo proteins (Ghosh and Kornfeld, 2003).

The medium subunit of the AP1 complex (μ subunit) was described to bind tyrosine-based sorting motifs, YXXφ, where X is any amino acid and φ is an hydrophobic amino acid (Rapoport et al., 1997; Carvajal-Gonzalez et al., 2012).

β-adaptin, one of the large subunits and one of the selected Y2H targets, was described as binding proteins with dileucine-based sorting motifs such as [DE]XXXL[LI] (Rapoport et al., 1998). In these motifs X represents any amino.

Given the biochemical evidence of an association between the NMIIA and β-adaptin we searched for the presence of these motifs in the amino acid sequence of NMIIA (Accession number: CAG30412.1). We found some tyrosine-based sorting motifs and interestingly one of these is located at tyrosine residue 158 marked in blue in Figure 25. Our group recently uncovered the phosphorylation of this residue by Src kinase upon infection with bacterial pathogen *L. monocytogenes*. This phosphorylation acts as a protection mechanism against *L. monocytogenes* invasion of host cells (Almeida et al., submitted).

NMIIA also contains two dileucine sorting motifs: the first at position 1232 and the second at position 1312. These two motifs are included in the tail fragment used as bait for the Y2H (Leu837 to Glu1960) (Figure 25). NMIIA sequences from different species were retrieved from GenBank (NCBI) (Species and Accession numbers are described on Table 6) and analyzed using MultAlin to check the conservation of the dileucine motifs. The two dileucine motifs were shown to be conserved among the higher taxonomic groups (Figure 26) strengthening the possibility that these motifs are essential to NMIIA function. The tyrosine motif is also conserved among all the analyzed species as was previously demonstrated by our group (Almeida et al., submitted).

The Y2H assay results plus the biochemical evidence suggesting an interaction between NMIIA and β-adaptin, the presence of these motifs in the NMIIA sequence and their conservation throughout the higher taxonomical groups allows us to speculate an interaction between the two proteins at a sequence level.

It is possible that NMIIA can bind both type of sorting motifs whether simultaneously or at different times is yet to be determined.

MAQQAADKYLYVDKNFINNPLAQADWAAKKLVWVPSDKSGFEPASLKEEVGEEAIVELVENGKKVKVNKDDIQKMNPPKFSKVEDMAELTCLNEASVLHNL
KERYYSGLIYTYSGLFCVVINPYKNLPIYSEEIVEMYKGKKRHEMPPHIYAITDTA**YRSM**MQDREDQSILCTGESGAGKTENTKKVIQYLAYVASSH
KSKKDQGELERQLLQANPILEAFGNAKTVKNDNSSRFGKFIRINFDVNGYIVGANIETYLLEKSRAIRQAKEERTFHIFYYLLSGAGEHLKTDLLLEPYNK
YRFLSNGHVTIPGQQDKDMFQETMEAMRIMGIPEEEQMGLLRVISGVLQLGNIVFKKERNTDQASMPDNTAAQKVSHLLGINVTDFTRGILTPRIKVGRDY
VQKAQTKEQADFAIEALAKATYERMFRWLVLRINKALDKTKRQGASFIGILDIAGFEIFDLNSFEQLCINYTNEKLQQLFNHTMFILEQEEYQREGIEWNF
IDFGLDLQPCIDLIEKPAGPPGILALLDEECWFPKATDKSFVEKVMQEQGTHPKFQKPKQLKDKADFCIIHYAGKVDYKADEWLMKNMDPLNDNIATLLHQ
SSDKFVSELWKDVDRIIGLDQVAGMSETALPGAFKTRKGMFRTVGQLYKEQLAKLMATLRNTNPNFVRCIIPNHEKKAGKLDPHLVLDQLRCNGVLEGIRI
CRQGFPNRVVFQEFRQRYEILTPNSIPKGFMDGKQACVLMIKALELDSNLYRIGQSKVFFRAGVLAHLEEERDLKITDVIIGFQACCRGYLARKAFAKRQQ
QLTAMKVLQRNCAAYLKLRNWQWWRLFTKVKP**LLQVSRQEEEMMAKEEELVKVREKQLAAENRLTEMETLQSQLMAEKLQLQEQLQAETELCAEAEELRAR
LTAKKQELEEICHDLEARVEEEEERCQHLQAEKKKMQQNIQELEEQLEEEESARQKLQLEKVTTEAKLKKLEEEQIILEDQNCKLAKEKKLLEDRIAEFTT
NLTEEEEKSKSLAKLKNKHEAMITDLEERLRREEKQRQELEKTRRKLEGDSTDLSDQIAELQAQIAELKMQLAKKEEELQAALARVEEEAAQKNMALKKIR
ELESQISELQEDLESERASRNKAEKQKRDLGEELEALKTELEDTLDSTAAQQELRSKREQEVNILKKTLEEEAKTHEAQIQEMRQKHSQAVEELAEQLEQT
KRVKANLEKAKQTLENERGELAN**EVKVLL**QGKGDSEHKRKKVEAQLQELQVKFNEGERVRTELADKVTKLQVELDNVTGLLSQSDSKSSKLTKDFS
ALESQLQ**DTQELL**QEENRQKLSLSTKLKQVEDEKNSFREQLEEEEEAKHNLEKQIATLHAQVADMKKKMEDSVGCLETAEEVKRKLQKDLEGLSQR
HEEKVAAYDKLEKTKTRLQQELDDLLVDLDHQRQSACNLEKKQKKFDQLLAEEKTISAKYAEERDRAEAEAREKETKALSLARALEEAMEQKAELERLNKQ
FRTEMEDLMSSKDDVGKSVHELEKSKRALEQQVEEMKTQLEELEDELQATEDAKLRLEVNLQAMKAQFERDLQGRDEQSEEKKKQLVRQVREMEAELEDER
KQRSMAVAARKKLEMDLKDLEAHIDSANKNRDEAIKQLRKLQAQMKDCMRELDDTRASREEILAQAKENEKKLKSMEAEMIQLQEELAAAERAKRQAQQER
DELADEIANSSGKGALALEEKRRLEARIAQLEEELEEEQGNTELINDRLKKANLQIDQINTDLNLERSHAQKNENARQQLERQNKELKVKLQEMEGTVKSK
YKASITALEAKIAQLEEQLDNETKERQAACKQVRRTEKKLKDVLLQVDDERRNAEQYKDQADKASTRLKQLKRQLEEAEEEAQRANASRRKLQRELEDATE
TADAMNREVSSLKNKLRRGDLPFVVPRRMARKGAGDGSDEEVDGKADGAEAKPAE

Figure 25 NMIIA heavy chain bioinformatic analysis. Amino acid sequence of the heavy chain of NMIIA. Tail fragment used as bait for the Y2H is highlighted in yellow. Tyrosine sorting motif at position 158, motor domain, is marked in blue and dileucine sorting motifs in the tail domain are marked in red.

Table 6 *In silico* analysis of dileucine sorting motifs in NMIIA. Comparative analysis of the NMIIA amino acid sequence from different species. Conserved dileucine motifs are shown in columns 3 and 4. Accession numbers for the amino acid sequences of NMIIA from the different species used are indicated.

Species	Accession Number	Dileucine Motif No.1	Dileucine Motif No.2
Homo sapiens	CAG30412.1	EVKVLL	DTQELL
Canis lupus familiaris	NP_001104237.1	EVKVLQ	DTQELL
Rattus norvegicus	NP_037326.1	EVKALL	DTQELL
Mus musculus	CAC85955.1	EVKALL	DTQELL
Gallus gallus	NP_990808.1	EVKVLL	DTQELL
Danio rerio	NP_001091647.2	ELKSLS	DAQALL
Caenorhabditis elegans	CAA92197.2	-	-
Drosophila melanogaster	AAB09050.1	-	EAQQLL
Dictyostelium discoideum	XP_637740.1	-	-
Saccharomyces cerevisiae	EDV09075.1	-	-

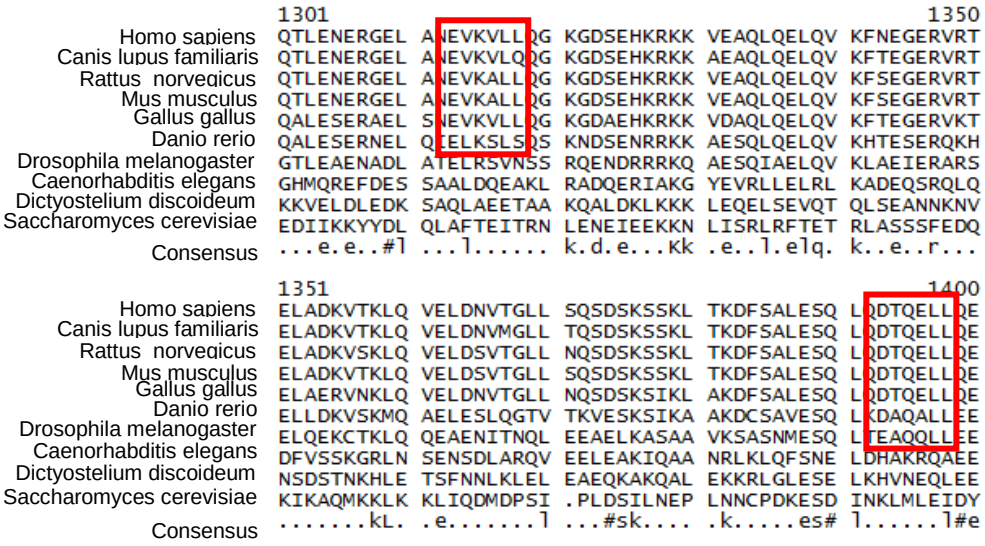

Figure 26 *In silico* analysis of dileucine sorting motifs in NMIIA using MultAlin. Amino acid sequences of NMIIA from different species were aligned and the presence of conserved dileucine motifs was determined. Conserved dileucine motifs between different species are shown in a red box.

4.9 Immunoprecipitation of β-Adaptin in Cos-7 cells ectopically expressing NMII chimeras

A preliminary experiment, performed only once, was designed in order to elucidate the possible binding of NMIIA to both subunits (μ and β) of the AP1 complex.

For this experiment we used Cos-7 cell expressing different GFP-tagged NMII chimeras: a NMII with the motor domain of NMIIB and the tail domain of NMIIA (NMIIB/A) and a NMII with the motor domain of NMIIA and tail domain of NMIIB (NMIIA/B).

Several tyrosine sorting motifs are present throughout the entire NMIIB amino acid sequence, both in the motor and tail domains. A dileucine motif was also identified at position 993 (Figure 27).

IP of β-adaptin was performed as described in section 4.7. As control we used GFP-tagged NMIIA that in agreement with our results associated with β-adaptin (Figure 24). In the blot only NMIIB/A was found associated with β-adaptin (Figure 28). This preliminary result suggests that AP1 only binds the tail of NMIIA.

MAQRTGLEDPERYLFVDRAVIYNPATQADWTAKKLVWIPSERHGFEAASIKEERGDEVMVELAENGKKAMVNKDDIQKMNPPKFSKVEDMAELTCLNEASV
LHNLKDRYYSGLIYTYSGLFCVVINPYKNLPIYSENIIEMYRGKKRHEMPPHIYAISESAYRCMLQDREDQSILCTGESGAGKTENTKKVIQYLAHVASSH
KGRKDHNIPESPKPVKHQGELERQLLQANPILESFGNAKTVKNDNSSRFGKFIRINFDVTGYIVGANIETYLLEKSRAVRQAKDERTFHIFYQLLSGAGEH
LKSDLLLEGFNNYRFLSNGYIPIPGQQDKDNFQETMEAMHIMGFSHEEILSMLKVVSSVLQFGNISFKKERNTDQASMPENTVAQKLCHLLGMNVMEFTRA
ILTPRIKVGRDYVQKAQTKEQADFAVEALAKATYERLFRWLVHRINKALDRTKRQGASFIGILDIAGFEIFELNSFEQLCINYTNEKLQQLFNHTMFILEQ
EEYQREGIEWNFIDFGLDLQPCIDLIERPANPPGVLALLDEECWFPKATDKTFVEKLVQEQGSHSKFQKPRQLKDKADFCIIHYAGKVDYKADEWLMKNMD
PLNDNVATLLHQSSDRFVAELWKDVDRIVGLDQVTGMTETAFGSAYKTKKGMFRTVGQLYKESLTKLMATLRNTNPNFVRCIIPNHEKRAGKLDPHLVLDQ
LRCNGVLEGIRICRQGFPNRIVFQEFRQRYEILTPNAIPKGFMDGKQACERMIRALELDPNLYRIGQSKIFFRAGVLAHLEEERDLKITDIIIFFQAVCRG
YLARKAFAKKQQQLSALKVLQRNCAAYLKLRHWQWWRVFTKVKPLLQVTRQEEELQAKDEELLKVKEKQTKVEGELEEMERKHQQLLEEKNILAEQLQAET

ELFAEAEEMRARLAAKKQELEEILHDLESRVEEEEERNQILQNEKKKMQAHIQDLEEQLDEEEGARQKLQLEKVTAEAKIKKM**EEEILL**LEDQNSK
FIKEKKLMEDRIAECSSQLAEEEEKAKNLAKIRNKQEVMISDLEERLKKEEKTRQELEKAKRKLDGETTDLQDQIAELQAQIDELKLQLAKKEEELQGALA
RGDDETLHKNNALKVVRELQAQIAELQEDFESEKASRNKAEKQKRDLSEELEALKTELEDTLDTTAAQQELRTKREQEVAELKKALEEETKNHEAQIQDMR
QRHATALEELSEQLEQAKRFKANLEKNKQGLETDNKELACEVKVLQQVKAESEHKRKKLDAQVQELHAKVSEGDRLRVELAEKASKLQNELDNVSTLLEEA
EKKGIKFAKDAASLESQLQDTQELLQEETRQKLNLSSRIRQLEEEKNSLQEQQEEEEEARKNLEKQVLALQSQLADTKKKVDDDLGTIESLEEAKKKLLKD
AEALSQRLEEKALAYDKLEKTKNRLQQELDDLTVDLDHQRQVASNLEKKQKKFDQLLAEEKSISARYAEERDRAEAEAREKETKALSLARALEEALEAKEE
FERQNKQLRADMEDLMSSKDDVGKNVHELEKSKRALEQQVEEMRTQLEELEDELQATEDAKLRLEVNMQAMKAQFERDLQTRDEQNEEKKRLLIKQVRELE
AELEDERKQRALAVASKKKMEIDLKDLEAQIEAANKARDEVIKQLRKLQAQMKDYQRELEEARASRDEIFAQSKESEKKLKSLEAEILQLQEELASSERAR
RHAEQERDELADEITNSASGKSALLDEKRRLEARIAQLEEELEEEQSNMELLNDRFRKTTLQVDTLNAELAAERSAAQKSDNARQQLERQNKELKAKLQEL
EGAVKSKFKATISALEAKIGQLEEQLEQEAKERAAANKLVRRTEKKLKEIFMQVEDERRHADQYKEQMEKANARMKQLKRQLEEAEEEATRANASRRKLQR
ELDDATEANEGLSREVSTLKNRLRRGGPISFSSSRSGRRQLHLEGASLELSDDDTESKTSDVNETQPPQSE

Figure 27 NMIIB heavy chain bioinformatic analysis. Amino acid sequence of the heavy chain of NMIIB. Dileucine sorting motif in the tail domain is marked in red.

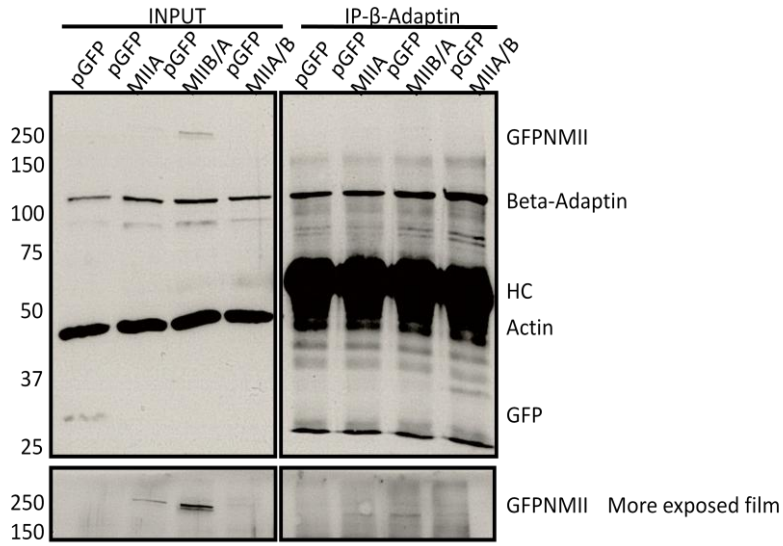

Figure 28 IP of β-adaptin in Cos-7 cells expressing GFP, GFP-NMIIA, GFP-NMIIB/A or GFP-NMIIA/B. Detection of actin protein levels was used as loading control. GFPNMII detection was achieved by immunoblot. GFP-NMIIA and GFP-NMIIB/A appear associated with β-adaptin in the IP fraction.

4.10 Intracellular localization of GFPMIIA, GFPMIIA-Y158F and β-adaptin in polarized Caco-2 cells

The medium subunit (μ) of AP1 was reported to sort Coxsackie Adenovirus Receptor (CAR) protein to the basolateral membrane of polarized cells through interaction with a tyrosine sorting motif (Diaz et al., 2009).

Phosphorylation of the tyrosine residue at position 158 by Src kinase in response to infection with bacterial pathogens was uncovered recently by our group. In the context of this study a mutant isoform of NMIIA, incapable of undergoing phosphorylation at tyrosine 158 (NMIIA-Y158F) was constructed (Almeida et al., submitted).

We hypothesized that wild-type NMIIA and the NMIIA-Y158F could have different intracellular locations or could affect the intracellular localization of β-adaptin in polarized Caco-2 cells.

To address that we used Caco-2 cells transiently expressing GFP-NMIIA and GFP-NMIIA-Y158F.

Caco-2 were allowed to polarize during 2, 6 and 10 days and processed for immunofluoresce analysis of Protein kinase C (aPKC, an apical marker) and NMIIA. Cells were also stained for actin and DNA. We observed bigger nucleus and a more diffuse staining for aPKC in cells that polarized for 2 days when comparing with cells allowed to polarize for 6 and 10 days (Figure 29a). Cells polarized for 6 days showed a more cohesive epithelium, smaller nucleus, and a more defined staining for both aPKC

and phalloidin, that appeared to surround the limit of the cell, suggesting polarization (Figure 29b). Caco-2 cells allowed to polarize for 10 days showed an epithelium with smaller nucleus, closer together than any of the other two conditions. aPKC and phalloidin presented a more distinct staining at the cell border, suggesting total polarization (Figure 29c). Considering these results we allowed Caco-2 cells to polarize for 10 days.

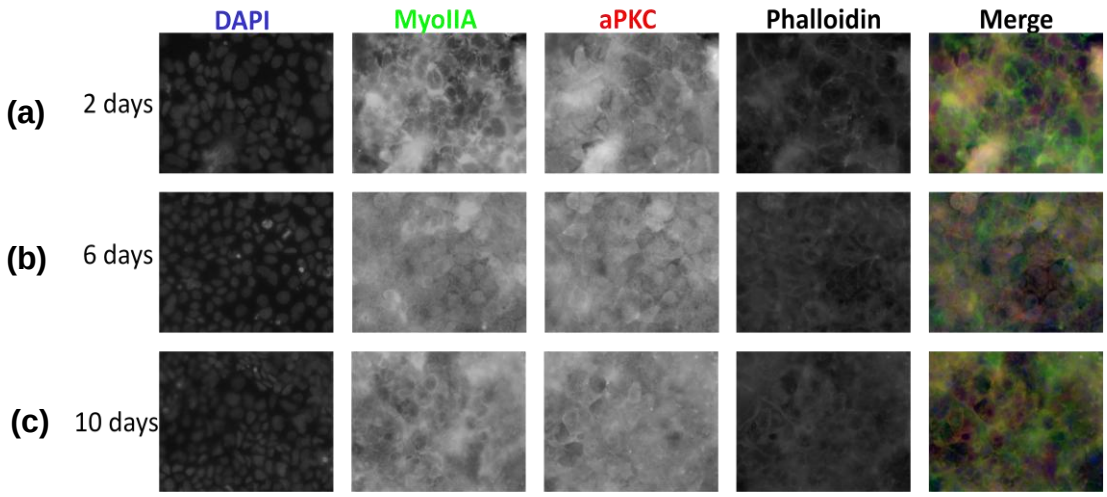

Figure 29 IF staining of Caco-2 cells allowed to polarize for different time periods, 2 days **(a),** 6 days **(b)** and 10 days **(c)**. Polarized Caco-2 cells were incubated with primary antibodies against NMIIA (green) and aPKC (red) and stained for actin (phalloidin, white) and DNA (DAPI, blue).

We then evaluated the role of NMIIA tyrosine phosphorylation in β-adaptin localization in polarized Caco-2 cells. Caco-2 cells were transfected to express GFP-NMIIA and GFP-NMIIA-Y158F and maintained under antibiotic selection. Through flow cytometry the population was selected (Figure 30). Only 1.2 % of cells expressed GFP-NMIIA and 1.8 % of cells expressed GFP-NMIIA-Y158F.

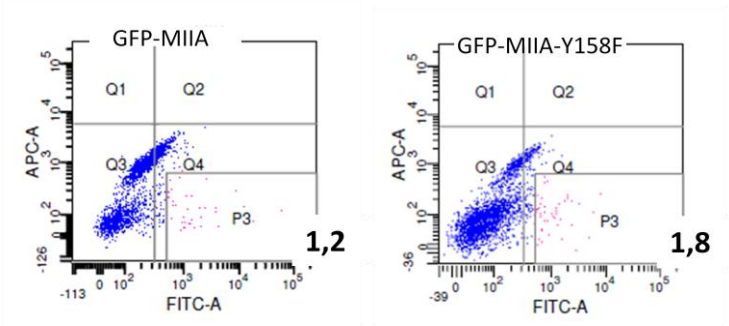

Figure 30 Results from the sorting of Caco-2 cells transiently expressing GFP-tagged NMIIA and GFP-tagged NMIIA-Y158F.

GFP-positive cells were seeded into a 96-well plate and expanded into a T75 flask. Cells were then seeded into TRANSWELL filters and maintained for 10 days to allow polarization. After 10 days filters were processed for IF analysis. Both aPKC and actin were localized at the border of the cell, suggesting that the epithelium is polarized (Figure 31A).

Caco-2 cells ectopically expressing GFP-WT-NMIIA and GFP-NMIIA-Y158F were incubated with primary antibodies against NMIIA and β-adaptin and stained for DNA (DAPI). NMIIA labeling was used because the levels of GFP-MIIA and GFP-MIIA-Y158F expression were very low and difficult to detect.

GFP-NMIIA-Y158F expressing cells seemed to have bigger nucleus with a bigger distance between them (Figure 31C) when compared to GFP-NMIIA cells (Figure 31B). β-adaptin appeared to have a more perinuclear localization in cells expressing GFP-NMIIA-Y158F (Figure 31C) when compared to GFP-NMIIA expressing cells. In cells expressing GFP-NMIIA the staining for β-adaptin seemed uniformely distributed in the cytoplasm (Figure 31B). In summary there seems to be a different epithelial organization between the two cell lines and β-adaptin seems to have a different localization inside the cell, however this is a preliminary experiment and needs to be repeated. In addition some controls are missing, enabling us to properly conclude what causes the observed differences in β-adaptin distribution and epithelium organization.

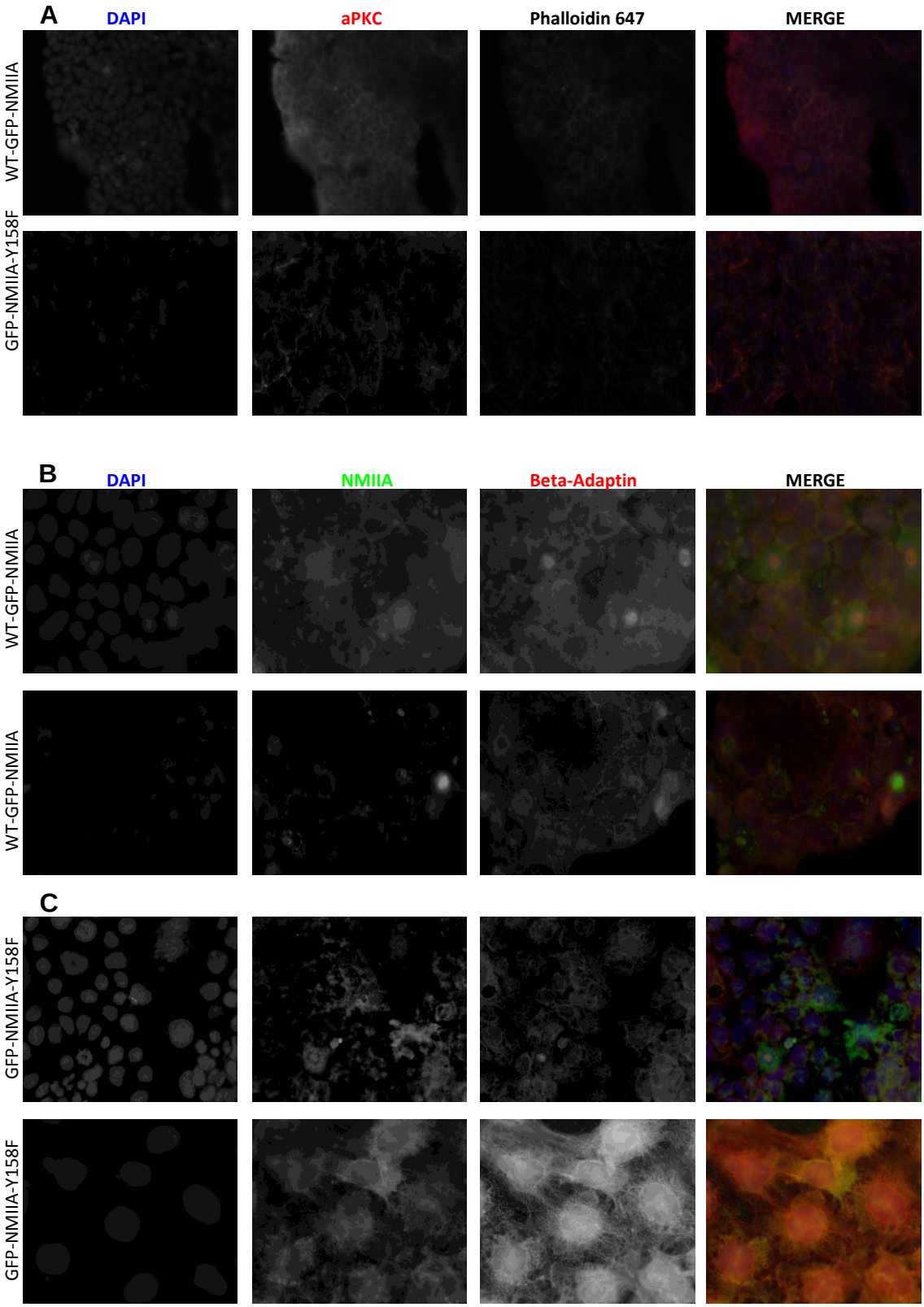

Figure 31 IF staining of polarized Caco-2 cells expressing GFP-NMIIA and GFP-NMIIA-Y158F. **(A)** Caco-2 cells expressing GFP-NMIIA and GFP-NMIIA-Y158F incubated with a primary antibody against aPKC, an apical marker, and stained for actin (phalloidin, white) and DNA (DAPI, blue). Cells were allowed to polarize for 10 days, after which they were processed for IF. **(B)** Caco-2 cells expressing GFP-NMIIA incubated with primary antibodies against NMIIA (green)

and β-adaptin (red) and stained for DNA (DAPI, blue). **(C)** Caco-2 cells expressing GFP-NMIIA-Y158F incubated with primary antibodies against NMIIA (green) and β-adaptin (red) and stained for DNA (DAPI, blue)

5. Discussion

5.1 Selection of the Y2H targets

Our group is focused on the study of cellular infectious process of the food-borne pathogen *L. monocytogenes.* Recently we showed the restrictive role of NMIIA in *L. monocytogenes* infection of host cells (Almeida et al., submitted).

Given that NMIIA has a relevant role in *L. monocytogenes* infection as well as in other infection processes like invasion of nonphagocytic cells by *Salmonella* (Hänisch et al., 2011), and viral entry of KSHV (Veettil et al., 2010) and HSV-1 (Arii et al., 2010), our group was interested to further investigating the role of NMIIA in infection and in canonical functions. In this context we searched for new NMIIA interacting partners. Through the realization of an Y2H screening 97 new NMIIA possible interacting partners were uncovered. The five chosen targets had PBS confidence ratings from A to D. These were: ZNF12 (A), SMPD4 (B), AFF1(C), β-adaptin and Hsp56 (D).

Selection of the target-proteins was based: on their PBS® and relevancy to the work performed in our laboratory.

The three highest ranked target-proteins of the screening were selected: ZNF12, SMPD4 and AFF1.

Eight other ZNF proteins were retrieved in the Y2H with ratings ranging from B to D. ZNF12 was chosen as representative for the remaining ZNFs. ZNFs are common contaminants in these types of screens due to their innate capacity of binding a protein through a single ZNF motif, producing unspecific interactions (Laity et al., 2001; Mackay and Crossley, 1998). Moreover all these proteins were poorly characterized and pre-existing information about them was obtained through bioinformatic sequence analysis.

Hsp56 and β-adaptin were chosen because of their possible links to *L. monocytogenes* pathogenesis.

Hsp56 was reported to interact with Hsp90 in a complex (Davies and Sánchez, 2005). Hsp90 is a Gp96 paralogue, which represents a major line of research in our group. Indeed, Gp96 was identified as a receptor for Vip, a *L. monocytogenes* virulence factor (Cabanes et al., 2005) and its subcellular localization is affected during infection (Martins et al., 2012).

The AP1 complex, of which β-adaptin is a subunit, is reported to be involved in the transport of CCVs inside the cell (Boehm and Bonifacino, 2001) while AP2 is mostly localized at the membrane and is responsible for endocytosis (Boehm and Bonifacino,

2001; McMahon and Boucrot, 2011). However, when large cargoes need to be internalized AP1 is described to localize at the membrane (McMahon and Boucrot, 2011). This complex was reported to be required for *L. monocytogenes* entry into host cells (Pizarro-Cerdá et al., 2007).

Although the Y2H assay is a powerful tool for a high-throughput screening results must be analyzed with precaution and a second platform should be used to validate the interactions (Dwane and Kiely, 2011).

5.2 Evaluation of the interactions between NMIIA and the five selected targets

To confirm the interactions between the selected targets and NMIIA we used a biochemical approach, IP. In this technique a protein is immunoprecipitated from a whole cell lysate using a specific antibody retrieving with it its interacting partners. When a protein is found to be associated with our immunoprecipitated protein we say that co-IP occurred (Dwane and Kiely, 2011).

Biochemical data did not allow the confirmation of the interactions between NMIIA and three of the selected target-proteins: ZNF12, SMPD4 and AFF1.

ZNF12 was detected by immunoblot in whole cell lysates (Figure 14E) but it never co-IP with NMIIA (Figure 18b).

SMPD4 has a predicted molecular weight of 93 kDa, a faint band above that molecular weight could be detected by the antibody specific against SMPD4 (Figure 18c). Even if the detected band corresponded to SMPD4 it never associated with NMIIA, when the latter was immunoprecipitated.

Finally, the antibody against AFF1 detected a very faint band in whole cell lysates from HeLa, HEK 293 and Jeg-3 (Figure 14A). In Figure 18a AFF1 is not detected in the INPUTs or in association with NMIIA in the IP fraction. We speculate that the expression levels of this protein could be very low.

From the five initially selected targets, these three were discarded either because it was difficult or not possible to detect the protein by immunoblot (AFF1) or because the protein could be detected in the whole cell lysate (ZNF12 and SMPD4) but it never co-IP with endogenous NMIIA in HeLa cells. Some other approaches should be tested in order to validate the interactions.

Alternatively to what was performed in the framework of this dissertation, the target proteins can be fused to a protein tag, overexpressed in cells and immunoprecipitated,

using an antibody specific for the tag. Commonly used tags include GFP, GST (Glutathione-S-transferase) and the FLAG-tag.

Another alternative could be the use of pull-down assays. Our protein of interest would be immobilized in a column where a cell lysate would pass through. Proteins with high affinity for the protein of interest would remain bound while the others would be washed through (Dwane and Kiely, 2011).

Concerning the remaining two targets (Hsp56 and β-adaptin), our results present biochemical evidence of an interaction with NMIIA.

IP of endogenous NMIIA (Figure 19) and Hsp56 (Figure 21A and 22A) both indicate a biochemical association between the two proteins. The role of this interaction will be addressed in the future.

Three different experimental designs suggest an association between NMIIA and β-adaptin. These were: IP of endogenous NMIIA (Figure 19), IP of β-adaptin (Figure 21B and 22B) and the IP of β-adaptin in Cos-7 cells expressing GFP-tagged NMIIA (Figure 24). In all three methods there was a recurrent biochemical association between the two proteins.

Reinforcing these results was the finding of tyrosine and dileucine sorting motifs present in the amino acid sequence of the heavy chain of NMIIA (Figure 25).

AP1 complexes sort proteins between intracellular compartments (Boehm and Bonifacino, 2001). This process occurs through binding of the μ subunit to tyrosine sorting motifs (Carvajal-Gonzalez et al., 2012 and Diaz et al., 2009) and binding of the β subunit to dileucine sorting motifs present in the cargo proteins (Rapoport et al., 1998).

Heavy chain of NMIIA possesses several tyrosine motifs. Interestingly, one of these motifs was located at position 158 (Figure 25). This tyrosine residue was recently uncovered by our group as capable of undergoing phosphorylation and playing a restrictive role upon *L. monocytogenes* infection (Almeida et al., submitted).

Two dileucine sorting motifs were found at positions 1232 and 1312 (Figure 25). Both motifs were located inside the NMIIA fragment used as bait for the Y2H assay (Figure 25).

Conservation of the tyrosine motif at position 158 among different species had already been reported (Almeida et al., submitted).

The two identified dileucine sorting motifs were also found to be conserved among the higher taxonomic groups (Figure 26).

The presence of these motifs in the sequence of NMIIA allows the speculation of an interaction between the two proteins at the sequence level. This coupled with the results from the Y2H assay and the data obtained from biochemical experiments indicates an association between β-adaptin and NMIIA.

A single experiment using NMII chimeras was performed, and suggests a possible specific binding of AP1 to the tail domain of NMIIA and therefore putatively to dileucine sorting motifs (Figure 28).

A molecular approach of site directed mutagenesis could be used to determine if NMIIA can bind both AP1 subunits.

To apply this technique it would be necessary to construct at least three different plasmids expressing different NMIIA isoforms with the different mutated sorting motifs to impair binding. Association between each of the NMIIA mutants and β-adaptin could be determined by IP.

Nevertheless the presence of these motifs in the NMIIA sequence, the conservation of the motifs among the higher taxonomic groups plus the biochemical results obtained strongly indicates an association between NMIIA and the AP1 complex, mainly β-adaptin.

5.3 Intracellular localization of WT-NMIIA, NMIIA-Y158F and β-adaptin in polarized Caco-2 cells

The NMIIA-Y158F isorform had its tyrosine 158 residue replaced by a phenylalanine and was therefore incapable of being phosphorylated (Almeida et al., submitted). Previous reports described that phosphorylation of a sorting motif in the target protein could either inhibit or enhance (Ghosh and Kornfeld, 2003) binding of the AP complex.

As a starting point to uncover a functional link between NMIIA and β-adaptin we decided to use polarized Caco-2 cells. Basolateral sorting of CAR in polarized cells occurs through the binding of the μ subunit of AP1 to a tyrosine motif in the protein (Diaz et al., 2009).

Caco-2 cells transiently expressing GFP-NMIIA and GFP-NMIIA-Y158F were seeded on TRANSWELL filters and allowed to polarize. We were capable of achieving polarization of the epithelium.

Cells expressing GFP-NMIIA present a more cohesive epithelium with smaller nucleus (Figure 31B) while cells expressing GFP-NMIIA-Y158F show bigger nucleus and a less organized epithelium (Figure 31C). This difference in epithelium organization could be

a result of altered NMIIA activity provoked by the inhibition of the phosphorylation of the Y158 residue.

A second difference could be observed in the distribution of β-adaptin. In cells expressing GFP-NMIIA the β-adaptin staining is mainly cytoplasmic (Figure 31B) while in cells expressing GFP-NMIIA-Y158F β-adaptin seems to be located closer to the nucleus, in a perinuclear distribution (Figure 31C).

In both cases quantifications were not performed so all possible conclusions are qualitative and further analysis are required.

In particular, Caco-2 cells transfected with a plasmid encoding only GFP, and IF stainings on untransfected polarized Caco-2 cells and untransfected non-polarized Caco-2 cells should be performed to allow interpretation of the obtained results.

Even though this experiment does not allows definitive conclusions it hints at a possible different epithelial organization and a possible difference in β-adaptin intracellular distribution between the two conditions.

6. Conclusions

Result from the Y2H screening plus biochemical data suggests an association of NMIIA and Hsp56. Both proteins appear to co-IP with the other.

Identification of a tyrosine motif at position 158 and two dileucine motifs, conserved among several species, in the NMIIA tail fragment used as bait for the Y2H allows the speculation of an interaction between NMIIA and and β-adaptin at the sequence level. This bioinformatic analysis coupled with the Y2H result and all the biochemical data obtained throughout this work strongly indicate an association between NMIIA and β-adaptin.

From the five target-proteins initially selected from the Y2H assay, we were not able to confirm the interaction of NMIIA with three of them (ZNF12, SMPD4 and AFF1) and showed that interaction occurs with the remaining two (Hsp56 and β-adaptin).

7. Bibliography

Alberts, B., Johnson, A., Lewis, J., Raff, M., Roberts, K. and Walter, P. (2008) Molecular Biology of the cell 5th Edition. New York: Garland Science.

Almeida M. T., Mesquita, F., Custódio, R., Cruz, R. Vingadassalom, D., Martins, M., Leong, J. M., Holden, D. W., Cabanes, D. and Sousa, S. (2013) Non-muscle Myosin Heavy Chain IIA is tyrosine phosphorylated by Src kinase upon infection and restricts intracellular levels of *Listeria monocytogenes*. *Cell Host & Microbe*, submitted.

Arii, J., Goto, H., Suenaga, T., Oyama, M., Kozuka-Hata, H., Imai, T., Minowa, A., Akashi, H., Arase, H., Kawaoka, Y. and Kawaguchi, Y. (2010) Non-muscle myosin IIA is a functional entry receptor for herpes simplex virus-1. *Nature* **476**: 859-864.

Betapudi, V. (2010) Myosin II Motor Proteins with Different Functions Determine the Fate of Lamellipodia Extension during Cell Spreading. *PLoS One* **5(1)**: e8560.

Betapudi, V., Licate, L. S. and Egelhoff, T. T. (2006) Distinct roles of non-muscle myosin II isoforms in the regulation of MDA-MB-231 breast cancer cell spreading and migration. *Cancer Res* **66**: 4725–4733.

Bitoun, E., Oliver, P. L. and Davies, K. E. (2006) The mixed-lineage leukemia fusion partner AF4 stimulates RNA polymerase II transcriptional elongation and mediates coordinated chromatin remodeling. *Human Molecular Genetics* **16(1)**: 92–106.

Boehm, M. and Bonifacino, J. S. (2001) Adaptins, the final recount. *Molecular Biology of the Cell* **12**: 2907–2920.

Bond, L. M., Brandstaetter, H., Sellers, J. M., Kendrick-Jones, J. and Buss, F. (2011) Myosin Motor Proteins are Involved in the Final Stages of the Secretory Pathways. *Biochem Soc Trans* **39(5)**: 1115–1119.

Bresnick, A. R. (1999) Molecular mechanisms of non-muscle myosin-II regulation. *Curr Opin Cell Biol* **11(1)**: 26-33.

Cabanes, D., Sousa, S., Cebriá, A., Lecuit, M. García-del Portillo, F. and Cossart, P. (2005) Gp96 is a receptor for a novel *Listeria monocytogenes* virulence factor, Vip, a surface protein. *The EMBO Journal* **24**: 2827-2838.

Cai, Y., Rossier, O., Gauthier, N. C., Biais, N., Fardin, M., Zhang, X., Miller, L. W., Ladoux, B., Cornish, V. W. and Sheetz, M. P. (2009) Cytoskeletal coherence requires myosin-IIA contractility. *Journal of Cell Science* **123**: 413-423.

Camejo, A., Carvalho, F., Reis, O., Leitão, E., Sousa, S. and Cabanes, D. (2011) The arsenal of virulence factors deployed by *Listeria monocytogenes* to promote its cell infection cycle. *Virulence* **2(5)**: 379-394.

Canobbio, I., Noris, P., Pecci, A., Balduini, A., Balduini, C. L. and Torti, M. (2005) Altered cytoskeleton organization in platelets from patients with MYH9-related disease. *J Thromb Haemost* **3(5)**: 1026-35.

Carvajal-Gonzalez- J. M., Gravotta, D., Mattera, R., Diaz, F., Perez Bay, A., Roman, A. C., Schreiner, R. P., Thuenauer, R., Bonifacino, J. S. and Rodriguez-Boulan, E. (2012) Basolateral sorting of the coxsackie and adenovirus receptor through interaction of a canonical YXXPhi motif with the clathrin adaptors AP-1A and AP-1B. *Proc Natl Acad Sci* **109(10)**: 3820-5.

Chambraud, B., Sardin, E., Giustiniani, J., Dounane, O., Schumacher, M., Goedert, M. and Baulieu, E. E. (2010) A role for FKBP52 in Tau protein function. *Proc Natl Acad Sci* **107**: 2658–2663.

Cioffi, D. L., Hubler, T. R. and Scammel, J. G. (2011) Organization and function of the FKBP52 and FKBP51 genes. *Curr Opin Pharmacol* **11(4)**: 308–313.

Conti, M. A., Even-Ram, S., Liu, C., Yamada, K. M. and Adelstein, R. S. (2004) Defects in cell adhesion and the visceral endoderm following ablation of nonmuscle myosin heavy chain II-A in mice. *The Journal of Biological Chemistry* **279**: 41263-41266.

Conti, M. A. and Adelstein, R. S. (2008) Nonmuscle myosin II moves in new directions. *J Cell Sci* **121(1)**: 11-8.

Cooper, G. M. (2000) The Cell: a molecular approach 2nd Edition. Sunderland (MA): Sinauer Associates.

Corcoran, C. A., He, Qin, Ponnusamy, S., Ogretmen, B., Huang, Y. and Sheikh, M. S. (2008) *Neutral Sphingomyelinase-3* Is a DNA Damage and Nongenotoxic Stress-Regulated Gene That Is Deregulated in Human Malignancies. *Mol. Cancer Res* **6(5)**: 795-807.

Cossart, P. (2011) Illuminating the landscape of host–pathogen interactions with the bacterium *Listeria monocytogenes*. *PNAS* **108(49)**: 19484-19491.

Cossart, P. and Toledo-Arana, A. (2008) *Listeria monocytogenes*, a unique model in infection biology: an overview. *Microbes and Infection* **10(9)**: 1041-1050.

Davies, T. H. and Sánchez, E. R. (2005) FKBP52. *The International Journal of Biochemistry & Cell Biology* **37**: 42-47.

Diaz, F., Gravotta, D., Deora, A., Schreiner, R., Schoggins, J., Falck-Pedersen, E. and Rodriguez-Boulan, E. (2009) Clathrin adaptor AP1B controls adenovirus infectivity of epithelial cells. *PNAS* **106(27)**: 11143-11148.

Dwane, S. and Kiely, P. A. (2011) Tools used to study how protein complexes are assembled in signaling cascades. *Bioengineered Bugs* **2(5)**: 247-259.

Formstecher, E., Aresta, S., Collura, V., Hamburger, A., Meil, A., Trehin, A., Reverdy, C., Betin, V., Maire, S., Brun, C., Jacq, B., Arpin, M., Bellaiche, Y., Bellusci, S., Benaroch, P., Bornens, M., Chanet, R., Chavrier, P., Delattre, O., Doye, V., Fehon, R., Faye, G., Galli, T., Girault, J. A., Goud, B., de Gunzburg, J., Johannes, L., Junier, M. P., Mirouse, V.,Mukherjee, A., Papadopoulo, D., Perez, F., Plessis, A., Rossé, C., Saule, S., Stoppa-Lyonnet, D., Vincent, A., White, M., Legrain, P., Wojcik, J., Camonis, J. and Daviet, L. (2005) Protein interaction mapping: a *Drosophila* case study. *Genome Res* **15(3)**: 376-84.

Gamsjaeger, R., Liew, C. K., Loughlin, F. E., Crossley, M. and Mackay, J. P. (2006) Sticky fingers: zinc-fingers as protein-recognition motifs. *TRENDS in Biochemical Sciences* **32(2)**: 63-70.

Ghosh, P. and Kornfeld, S. (2003) AP-1 binding to sorting signals and release from clathrin-coated vesicles is regulated by phosphorylation. *The Journal of Cell Biology* **60(5)**: 699–708.

Giorgini, F. and Muchowski, P. J. (2005) Connecting the dots in Huntington's disease with protein interaction networks. *Genome Biology* **6**: 210.

Grantham, J., Lassing, I. and Karlsson, R (2012) Controlling the cortical actin motor. *Protoplasma* **249**: 1001-1015.

Hänisch, J., Kölm, R., Wozniczka, M., Bumann, D., Rottner, K. and Stradal T. E. (2011) Activation of a RhoA/myosin II-dependent but Arp2/3 complex-independent pathway facilitates *Salmonella* invasion. *Cell Host Microbe* **9(4)**: 273-85.

Heissler, S. M. and Manstein, D. J. (2013) Nonmuscle myosin-2: mix and match. *Cell Mol Life Sci* **70**: 1–21.

Helfand, B. T., Chang, L., and Goldman, R. D. (2003) The dynamic and motile properties of intermediate filaments. *Annu Rev Cell Dev Biol* **19**: 445-67.

Ihrke, G., Kyttälä, A., Russel, M. R. G., Rous, B. A. and Luzio, J. P. (2004) Differential Use of Two AP-3-mediated Pathways by Lysosomal Membrane Proteins. *Traffic* **5**: 946–962.

Karcher, R. L., Deacon, S. W. and Gelfand, V. I. (2002) Motor–cargo interactions: the key to transport specificity. *TRENDS in Cell Biology* **12(1)**: 21-27.

Laity, J. H., Lee, B. M. and Wright, P. E. (2001) Zinc finger proteins: new insights into structural and functional diversity. *Current Opinion in Structural Biology* **11**: 39-46.

Landsverk, M. L. and Epstein, H. F. (2005) Genetic analysis of myosin II assembly and organization in model organisms. *Cell Mol Life Sci* **62(19-20)**: 2270-82.

Loubéry, S. and Coudrier, E. (2008) Myosins in the secretory pathway: tethers or transporters? *Cell Mol Life Sci* **65**: 2790–2800.

Mackay, J. P. and Crossley, M. (1998) Zinc fingers are sticking together. *TIBS* **23**.

Martins, M., Custódio, R., Camejo, A., Almeida, T. M., Cabanes, D. and Sousa, S. (2012) *Listeria monocytogenes* triggers the cell surface expression of Gp96 protein and interacts with its N terminus to support cellular infection. *J Biol Chem* **287(51)**: 43083-93.

McMahon, H. T. and Boucrot, E. (2011) Molecular mechanism and physiological functions of clathrin-mediated endocytosis. *Nature Reviews, Molecular Cell Biology* **12**: 517-533.

Moser, J. J., Chan, E. K. L. and Fritzler, M. (2009) Optimization of immunoprecipitation–western blot analysis in detecting GW182-associated components of GW/P bodies. *Nature Protocols* **4(5)**: 674–685.

Müsch, A., Cohen, D. and Rodriguez-Boulan, E. (1997) Myosin II Is Involved in the Production of Constitutive Transport Vesicles from the TGN. *The Journal of Cell Biology* **138(2)**: 291–306.

Petrosyan, A., Ali, M. F., Verma, S. K., Cheng, H. and Cheng, P. (2012) Non-muscle myosin IIA transports a Golgi glycosyltransferase to the endoplasmic reticulum by binding to its cytoplasmic tail. *The International Journal of Biochemistry & Cell Biology* **44**: 1153-1165.

Pizarro-Cerdá, J., Payrastre, B., Wang, Y., Veiga, E., Yin, H. L. and Cossart, P. (2007) Type II phosphatidylinositol 4-kinases promote *Listeria monocytogenes* entry into target cells. *Cellular Microbiology* **9(10)**: 2381–2390.

Rain, J.C., Selig, L., De Reuse, H., Battaglia, V., Reverdy, C., Simon, S., Lenzen, G., Petel, F., Wojcik, J., Schächter, V., Chemama, Y., Labigne, A. and Legrain, P. (2001) The protein-protein interaction map of *Helicobacter pylori*. *Nature* **409(6817)**: 211-5.

Rapoport, I., Chen, Y. C., Cupers, P., Shoelson, S. E. and Kirchhausen, T. (1998) Dileucine-based sorting signals bind to the β chain of AP-1 at a site distinct and

regulated differently from the tyrosine-based motif-binding site. *The EMBO Journal* **17(8)**: 2148-2155.

Rapoport, I., Miyazaki, M., Boll, W., Duckworth, B., Cantley, L. C., Shoelson, S. and Kirchhausen, T. (1997) Regulatory interactions in the recognition of endocytic sorting signals by AP-2 complexes. The *EMBO Journal* **16**: 2240–2250.

Scammell, J. G., Hubler, T. R., Denny, W. B. and Valentine, D. L. (2003) Organization of the human FK506-binding immunophilin FKBP52 protein gene (FKBP4). *Genomics* **81**: 640–643.

Sellers, J. R. (2000) Myosins: a diverse superfamily. *Biochimica et Biophysica Acta* **1496**: 3-22.

Sivils, J. C., Storer, C. L., Galigniana, M. D. and Cox, M. B. (2011) Regulation of Steroid Hormone Receptor Function By the 52-kDa FK506-Binding Protein (FKBP52). *Curr Opin Pharmacol* **11(4)**: 314–319.

Spector, D. L. and Lammond, A. I. (2011) Nuclear speckles. *Cold Spring Harb Perspect Biol* **3(2)**: a000646.

Vazhappilly, R., Wee, K. S., Sucher, N. J. and Low, C. M. (2010) A non-muscle myosin II motor links NR1 to retrograde trafficking and proteasomal degradation in PC12 cells. *Neurochem Int* **56(4)**: 569-76.

Veettil, M. V., Sadagopan, S., Kerur, N., Chakraborty, S. and Chandran, B. (2010) Interaction of c-Cbl with Myosin IIA Regulates Bleb Associated Macropinocytosis of Kaposi's Sarcoma-Associated Herpesvirus. *PLoS Pathogens* **6(12)**: e1001238

Vicente-Manzanares, M., Ma, X., Adelstein, R. S. and Horwitz, A. R. (2009) Non-muscle myosin II takes centre stage in cell adhesion and migration. *Nat Rev Mol Cell Biol* **10(11)**: 778-790.

Wang, A., Ma, X., Conti, M. A. and Adelstein, R. S. (2011) Distinct and redundant roles of the non-muscle myosin II isoforms and functional domains. *Biochem Soc Trans* **39(5)**: 1131-5.

Zhang, Y., Conti, M. A., Malide, D., Dong, F., Wang, A., Shmist, Y. A., Liu, C., Zerfas, P., Daniels, M. P., Chan, C., Kozin, E., Kachar, B., Kelley, M. J., Kopp, J. B. and Adelstein, R. S. (2011) Mouse models of *MYH9*-related disease: mutations in nonmuscle myosin II-A. *Blood* **119(1)**: 238-50.


U.PORTO
FACULDADE DE CIÊNCIAS
UNIVERSIDADE DO PORTO